Spring 5-4-2024

Selective Separation of Metal Ions from Aqueous Process Streams Using Magnetite Adsorbent

Daniel Geottlich

Selective Separation of Metal Ions from Aqueous Process Streams Using Magnetite Adsorbent

by

Goettlich Daniel

A thesis submitted in partial fulfillment of the requirements for the degree of

Materials Science and Engineering

Montana Tech

2024

Abstract

The effect of coexisting ions on the selectivity of adsorption onto magnetite nanoparticles (MNPs) for various elements in aqueous solutions was investigated. Surrogate solutions of varying concentrations of rare earth elements (REEs), heavy metals, and gangue elements (low commercial value elements or metals) were mixed with MNPs. Selectivity experiments were performed on surrogate samples based on the composition of a REE ore concentrate and a leach liquor from the chlorinated products of the roasted REE ore concentrate. Adsorption efficiency of magnetite was determined by measuring ion concentration in a sample using inductively coupled plasma-optical emission spectroscopy (ICP-OES). Magnetite is selective towards Cr(III) over some of the REEs and metals; this behavior can be controlled by adjusting the pH and MNP dosage. Rare earth experiments show that Sc(III) is selective over other REEs at a pH of 5.3. The REE ore sample and surrogate experiments reveal that magnetite will preferentially adsorb iron over REEs depending on the pH; where iron adsorption efficiency was significantly higher than the REEs at a pH of 2.5 and 4.5. By varying the MNP concentration, it appears plausible that a multi-stage extraction process could use the selectivity trends determined by this study to effectively target extraction of chromium, scandium, and iron.

Keywords: magnetite, selectivity, water purification, rare earth elements

Dedication

For the support, love, and prayers, of my friends and family who made this accomplishment possible. In honor of my grandfather, Anthony Inverso (1937 – 2008), who inspired me to pursue a career in science.

Acknowledgements

My appreciation and thanks to the Dr. Downey research team for their expertise and advice in designing experiments. To Dr. Downey for taking me into his research team and giving me an opportunity to complete my masters along with his knowledge, guidance, and patience. To my committee members, Dr. Teagan Leitzke and Gary Wyss, for Teagan helping with getting started in MNP research (from experiment procedure to experiment design) and Gary's assistance in operating the ICP instrument and repairing it. A thank you to Dr. Grant Wallace for helping with experiment setup. Katie Schumacher for her help in the REE ore chloride roasting. Maureen Chorney for assisting me with the ICP work. Trevor Russel for helping in the analysis of data and research suggestions. Abdul Sommed Hadi for his advice and friendship. This project was funded by the National Science Foundation EPSCoR Cooperative Agreement OIA-1757351. Any opinions, findings, and conclusions or recommendations expressed in this material are those of the author(s) and do not necessarily reflect the views of the National Science Foundation.

Table of Contents

List of Tables

List of Figures

List of Equations

Glossary of Terms

- **REE**: Rare earth Elements
- **RECl:** Rare Earth Chloride
- **REOCl**: Rare earth Oxychloride
- **MNPs:** Magnetite Nanoparticles
- **ICP-OES:** Inductively Coupled Plasma Optical Emission Spectroscopy
- **CFMR:** Continuous Flow Material Recovery
- **IX:** Ion Exchange

1. Introduction

1.1. Background on contaminated waters

Clean and affordable water is vital to grow and sustain populations. However, environmental issues are burgeoning due to years of technological and industrial expansion environmental issues, particularly water pollution. The effluent from industrial processes contains concentrations of heavy metals that require treatment in order to be safely discharged into the environment. In addition, valuable heavy metals, or elements such as the rare earth elements (REEs) provide an economic incentive for their extraction and recovery. Efficient and environmentally safe treatment of industrial effluent would greatly benefit from the availability of a means of on-site recovery of valuable and toxic metals to avoid waste transportation costs and dangers.

Heavy metals are typically classified as elements with high densities or atomic numbers (having an atomic number greater than 20 and a density of at least 5 g/cm^3) and are typically toxic in low concentrations. Cadmium, chromium, copper, and cobalt are the heavy metals

investigated in this study because of their toxicity from human, aquatic, and environmental perspectives but also their worth and value from an economic perspective.

Cadmium is a toxic heavy metal, commonly found in zinc ores and as a byproduct of zinc mining operations. Many industrial applications have been found for cadmium, including Ni-Cd batteries, paint and plastic pigments, and plastic stabilizers[1]. In addition, due to its anti-corrosive properties, cadmium is used in electroplating and galvanizing alloys. However, cadmium is toxic to humans, plants, and wildlife as well as a potent carcinogen and teratogen[2]. Exposure to the environment from industrial effluent and wastewater can lead to accumulation in the soil from which uptake by leafy plants results in cadmium-contaminated vegetable and wildlife resources[1].

Chromium is used in a wide variety of industrial applications and processes including chrome plating, leather tanning, stainless steel production and welding[1]. Increased chromium levels within the environment are the result of widespread industrial use, occurring in wastewater in trivalent and hexavalent forms[1]. Hexavalent chromium is carcinogenic and toxic to ecosystems. Although trivalent chromium poses significantly less risk in trace levels (it is an essential metal for normal physiological function), it can be oxidized to its hexavalent state in natural waters[2]. The removal of trivalent and hexavalent chromium from wastewaters is critical.

A ferromagnetic transition metal used in permanent magnets, catalysts, and other industrial applications such as the production of cemented carbides, cobalt is an important metal in modern industry[1], [3], [4]. Cobalt pollution in soil and water occurs primarily from areas near factories and heavily industrialized cities but can also enter the environment from mining activities. Chronic exposure to cobalt can cause adverse health effects such as neurological,

cardiovascular, and endocrine deficits. Cobalt extraction and removal from waste waters would be beneficial both economically and environmentally.

Removal of copper from wastewater is important as well because many aquatic species are particularly sensitive to copper exposure, which can cause severe liver, kidney, and respiratory damage. Acute exposure to copper via ingestion causes nausea, vomiting, and abdominal pain in humans. Copper exposure sources are commonly the result of contaminated beverages, food, or drinking water. Chronic exposure of copper to humans in drinking water can cause mental illnesses[1].

A summary of the economic value and demand of heavy metals of interest in this study are presented in Table 1[5].

Table 1: Summary of economic value, production, and demand of heavy metals[5].

[illegible]	[illegible]			[illegible]		
[illegible]	[illegible]	[illegible]	[illegible]	[illegible]	[illegible]	[illegible]
[illegible]	[illegible]	[illegible]	[illegible]	[illegible]	[illegible]	[illegible]
[illegible]	[illegible]	[illegible]	[illegible]	[illegible]	[illegible]	[illegible]
[illegible]	[illegible]	[illegible]	[illegible]	[illegible]	[illegible]	[illegible]
[illegible]	[illegible]	[illegible]	[illegible]	[illegible]	[illegible]	[illegible]
[illegible]	[illegible]			[illegible]		
[illegible]	[illegible]	[illegible]	[illegible]	[illegible]	[illegible]	[illegible]
[illegible]	[illegible]	[illegible]	[illegible]	[illegible]	[illegible]	[illegible]
[illegible]	[illegible]	[illegible]	[illegible]	[illegible]	[illegible]	[illegible]
[illegible]	[illegible]	[illegible]	[illegible]	[illegible]	[illegible]	[illegible]
[illegible]	[illegible]	[illegible]	[illegible]	[illegible]	[illegible]	[illegible]
[illegible]	[illegible]					
[illegible]	[illegible]	[illegible]	[illegible]			
[illegible]	[illegible]	[illegible]	[illegible]			
[illegible]	[illegible]	[illegible]	[illegible]			
[illegible]	[illegible]	[illegible]	[illegible]			
[illegible]	[illegible]	[illegible]	[illegible]			

Further, rare earth element exposure to the environment and humans will occur more often as the demand for these elements increases [6]. Rare earth elements are known to not volatilize, degrade, or metabolize in the environment but have been known to bioaccumulate in seaweed[7]. The biological effects of short-term exposure to humans are not well understood[8], but the long-term biological effects of exposure to humans can lead to accumulation in the bone tissue and cause genetic toxicity [9]. Due to their immense economic value and potential adverse

effects on environmental and human health, it is important to remove and recover rare earth elements from industrial effluent and wastewater. Table 2 displays the prices of rare earth element oxides from 2021[10].

Table 2: Rare earth element oxides prices in US $/kg[10].

Compound	Price (US$/kg)
CeO_2	2
La_2O_3	2
Nd_2O_3	47
Y_2O_3	3
Pr_6O_{11}	75
Sm_2O_3	6
Gd_2O_3	24
Dy_2O_3	180
Sc_2O_3	3800

1.2. Background on water purification and magnetite

A wide variety of options are available to treat metal contaminated wastewaters and each method has its own advantages and disadvantages. The most common wastewater treatment techniques are chemical precipitation, ion exchange (IX), and adsorption. Each technique is described below:

The most common wastewater metal removal technique is chemical precipitation where the metal ion of interest reacts with a precipitant – such as carbonates, sulfides, or most commonly, hydroxides -to produce an insoluble product. Precipitation with lime is often used due to its low cost, availability, and potency for high quantities of metals. However, large doses of precipitants require an extensive reaction time and produce excessive sludge waste that does not allow for ease of metal recovery and has long term environmental consequences[11], [12], [13].

Ion-exchange involves a solid phase, insoluble media that exchanges metal ions in an aqueous solution for ions in the media. A great number of materials for ion-exchange media are available, and examples include natural materials like zeolite or synthetic resins. These materials can be enhanced with functional groups to improve ion selectivity or provide a greater number of sites for ion exchange. Major disadvantages of ion exchange are the media are prone to fouling against highly concentrated solutions, batch processing leads to difficulty for use in large-scale operations and the process requires considerable effort to operate and maintain[11], [12].

Adsorption employs solid phase adsorbents to collect ions, also called adsorbates, present in an aqueous solution. The ions collect on the surface of the material by chemisorption (chemical bonding between the ion and adsorbent) or physisorption (weak molecular interactions such as van der Waals forces). Adsorbent material options such as activated carbon or magnetite (Fe_3O_4) are widely available, cost effective, and environmentally compatible[11], [14]. Advantages include ease of removal of loaded adsorbent from effluent streams, ability to recover or discard the removed metals in an additional step if desired, and to a variety of solution conditions in small or large-scale operations, and batch, or continuous-flow processes. Disadvantages are the limited number of active sites for adsorption and lack of ion selectivity[11], [13], [14], [15].

Magnetite was selected as adsorbent for this research for the following reasons:

- Proven viability in an industrially applicable system, the Continuous Flow Material Recovery system (CFMR), a project that has been well-developed from previous studies at Montana Tech[11].
- Nanoparticle magnetite (10-30 nm) are superparamagnetic; the magnetic properties allow for ease of separation from effluent streams once loaded with contaminants[16], [17].

- Versatility with a variety of ions in cationic or anionic states[13], [16]
- Colloidal stability and capability to be augmented with ligand functional groups onto the magnetite surface to tune ion affinity[11], [18].

One application for the research described in this study is use with the CFMR system. Figure 1 depicts the configuration of the third-generation iteration of the CFMR system.

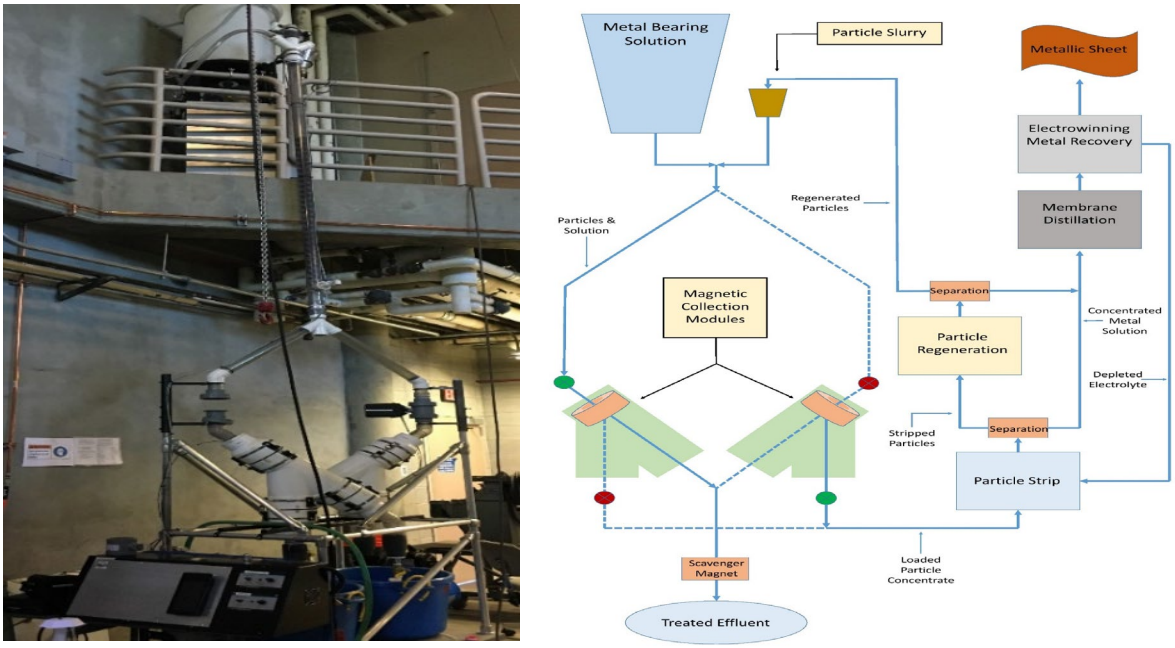

Figure 1: Third generation continuous flow reactor system. Pilot-sale dual column continuous flow reactor (left). Flow diagram of the third-generation dual column reactor (right) [19]**.**

The CFMR system provides a simple and economical method to treat contaminated water using magnetite in a continuous system that can be adapted to large- or small-scale operations. Initial CFMR system development began in 2004 under the collaboration of Dr. Downey, then at Hazen Research Inc. (Golden, Colorado), and Dr. Arijit Bose of the University of Rhode Island and later Dr. Rosenberg of the University of Montana. The design of the system expanded under the research Dr. Hutchins of Montana Tech[20] and has been improved upon by others

throughout the years. Dr. Leitzke, of Montana Tech, defined the adsorptive capacities of magnetite for copper, lead, and phosphate under the specified conditions[21] [22]. Work done by M.S, T. Russel, studied the regeneration of the stripping solution using copper surrogate solutions. Previous research has validated its potential for use within the industrial sector for metal removal and recovery[11], [21], [22].

An illustration of the setup for the 5th generation CFMR system is shown in Figure 3[21].

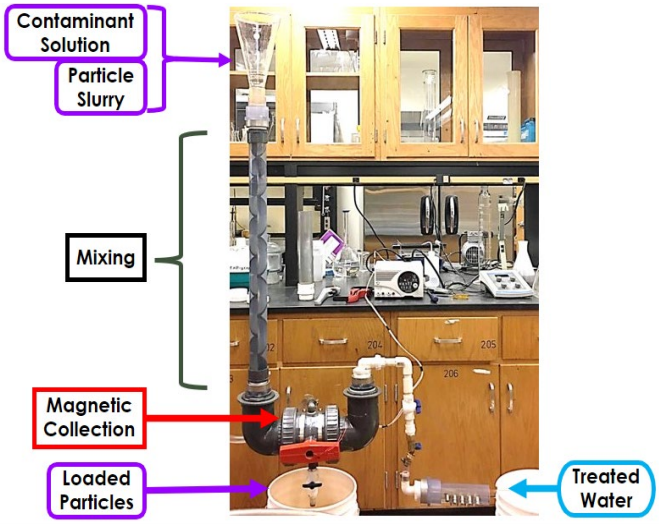

Figure 2: 5th generation CFMR experimental setup[21].

A detailed description and depiction of the CFMR system process is shown in Figure 3.

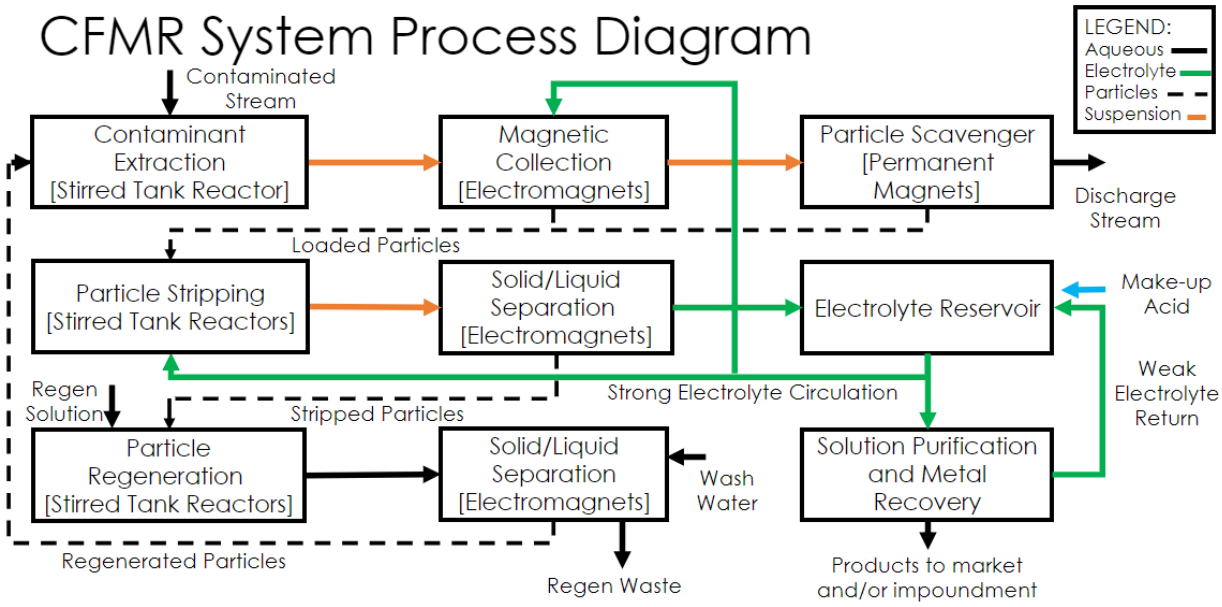

Figure 3: 5th generation CFMR system process flow diagram with detailed descriptions[22].

While significant progress has been made, in terms of understanding ion adsorption on MNPs, most prior research focused on overall adsorption of ions contained in single element solutions or in the multi-element solution experiments, with little emphasis on the effects of coexisting ions on magnetite adsorption. Two interrelated purposes of this project were to investigate how selectivity affects the uptake of multiple elements, and to further develop the CFMR technology by improving the understanding of the effects of coexisting ions on magnetite adsorption.

The prominent factors of selectivity are determined by radius and charge density of the target ion. Generally, larger ions with higher valence states have a greater affinity for adsorption than smaller ions with a lower valence state. Ions of the same charge can have greater affinity than others due to a smaller ionic radius and increased tendency to accept electrons (Lewis acidity). Information on the ionic radii and ionic state of elements relevant to this study are presented in Table 3[20].

Table 3: Tabulation of ionic radii and valence state of elements selected for this study[23].

Element	Ionic radius (nm)	Ionic charge
Al	**0.05**	**3**
Ca	**0.099**	**2**
Sc	**0.081**	**3**
Cr	**0.075**	**3**
Mn	**0.082**	**2**
Fe	**0.077**	**2**
Co	**0.072**	**2**
Cu	**0.071**	**2**
Zn	**0.074**	**2**
Y	**0.093**	**3**
Cd	**0.097**	**2**
La	**0.115**	**3**
Ce	**0.115**	**3**
Eu	**0.108**	**3**
Gd	**0.108**	**3**
Tb	**0.106**	**3**
Dy	**0.105**	**3**
Er	**0.103**	**3**
Tm	**0.102**	**3**
Yb	**0.101**	**3**

The surface of adsorption media can be altered with ligands to enable the selective uptake of target ions by the formation of metal complexes. Research involving magnetite nanoparticles for the selective uptake of target ions uses functionalized or ligand incorporated MNP media. The selectivity of virgin MNPs, has not been the subject of significant research.

1.3. The effect of coexisting ions on magnetite adsorption

Understanding the effects of coexisting ions on the adsorption of specific target ions is critical for the future development and application of magnetite as an adsorbent. A concern with the majority of past research on magnetite is that few studies are directed solely to understanding which ions will preferentially be adsorbed. In most previous magnetite adsorption research, experiments focused primarily on the adsorption capability using single element surrogate solutions or multi-element solutions, leaving an understanding of ion selectivity ambiguous. Adsorption selectivity is important because industrial wastewater will contain an array of metals, and some are considerably more valuable than others. It would be highly beneficial both economically and environmentally to be able to sequester and concentrate the metals of higher value or the metals of greater environmental concern from the others for ease of refining or disposal.

The influence of coexisting ions on adsorption is complex, and capable of aiding or inhibiting adsorption capacity in a multitude of ways- including competing adsorption sites, weakening electrostatic interactions, formation of ion pairs, changing the total number of adsorption sites, and transforming adsorbate particle size. Parameters such as contact time, concentration, and solution pH are salient factors in adsorption selectivity changes. Selectivity of rare earth elements from other rare earths is particularly important and an area of research with great interest.

Selectivity Values are notoriously inconsistent and vary depending on the adsorbent medium and the relative concentrations of different ionic species, among other factors. As a result, numerical selectivity values reported in the literature are also inconsistent and, therefore, approximate values are considered adequate for process screening [24]. Selectivity can be defined as a ratio relative to the changing concentrations of the ions of interest at equilibrium

within an aqueous solution[25], [26], [27]. For the purpose of this study, selectivity will be defined as the ratio distribution of selectivity coefficients of coexisting ions described by equations 1 and 2[25], [27]:

$$K_d(\,mL \cdot g^{-1}) = \frac{(\,Co-Ce\,)}{Ce} \cdot \frac{V}{m} \qquad 1)$$

$$K_{Mi/Mii} = \frac{K_d^{Mi}}{K_d^{Mii}} \qquad 2)$$

where C_0 represents the initial ion concentration, and $Ce\ (mmol\ L^{-1})$ represents the equilibrium (final) ion concentration; $V\ (mL)$ is the solution volume and $m\ (g)$ is the mass of the magnetic adsorbent. Selectivity coefficients $(K_{Mi/Mii})$ were estimated as the ratio distribution coefficient of *Mi* (the element with the highest selectivity coefficient, K_d, for a given experiment) to the distribution coefficient of coexisting ions, M_{ii}.

1.4. Background on rare earths

Rare earth elements have been called the “vitamins of a modern economy” or “the engine of electronification and the seeds of technology”. They are of paramount importance to many of the industries that drive modern technology. Many common technological devices, cellphones and the magnets used in car and airplanes, use rare earth elements, and they are vital to sustaining and growing green technology, in addition to their need in multitudinous applications for military technology[28], [29]. They are also critical to smartphone technology, particularly in the screen and speakers as presented in Figure 4. Lanthanum is used extensively in the camera lenses and screen display while the magnets used are primarily composed of neodymium-iron-boron (NdFeB) [28], [30].

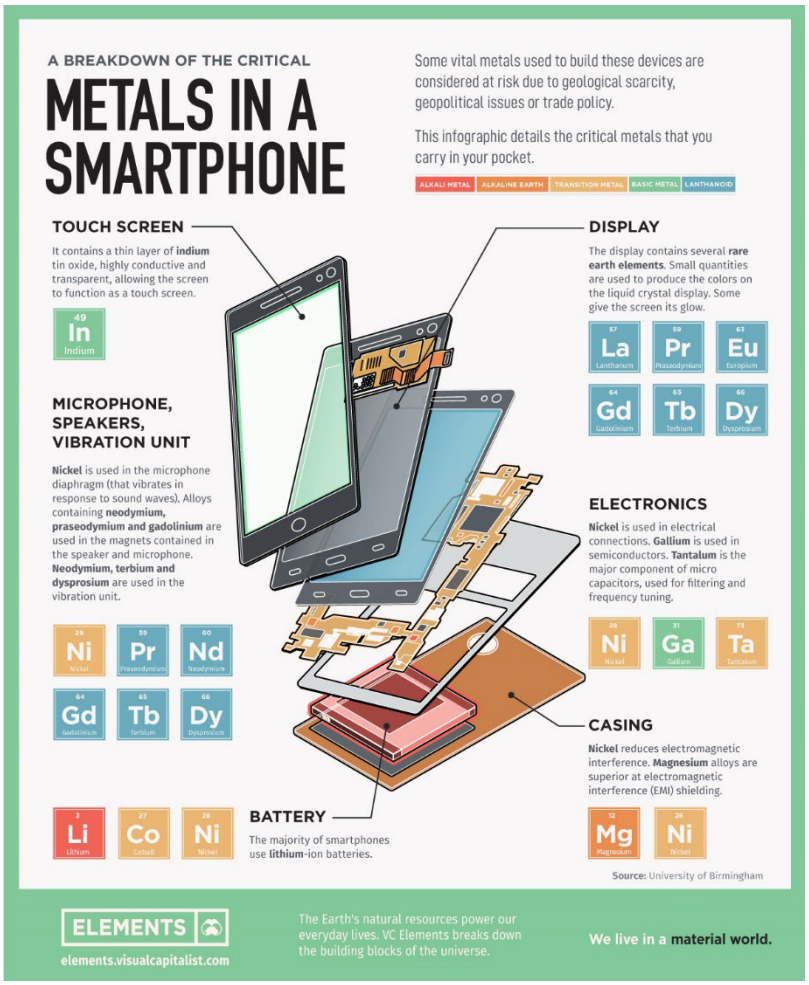

Figure 4: End applications of rare earth elements in smartphones[30].

The most powerful (neodymium-iron-boron, NeFeB) and most corrosion and heat resistant (samarium-cobalt) magnets are composed of rare earth alloys. Samarium-cobalt magnets are necessary components in high-speed motors and generators in cars and airplanes because they are among the few magnets able to function in high temperature environments. Neodymium magnets are the strongest magnets currently available and have applications in a variety of critical technologies such as multi-gigabyte portable disc drives and military components[28], [29].

The demand for neodymium magnets and rare earth alloys is expected to increase drastically in future years, yet their supply and price is not stable[28], [29], [31]. The United States currently has little domestic production of rare earth metals and is vulnerable to the foreign-dominated rare earths supply chain [29], [31]. The mining of rare earths has decentralized away from China within recent years, although they still possess the majority of the world's facilities for processing of rare earths[29], [31].

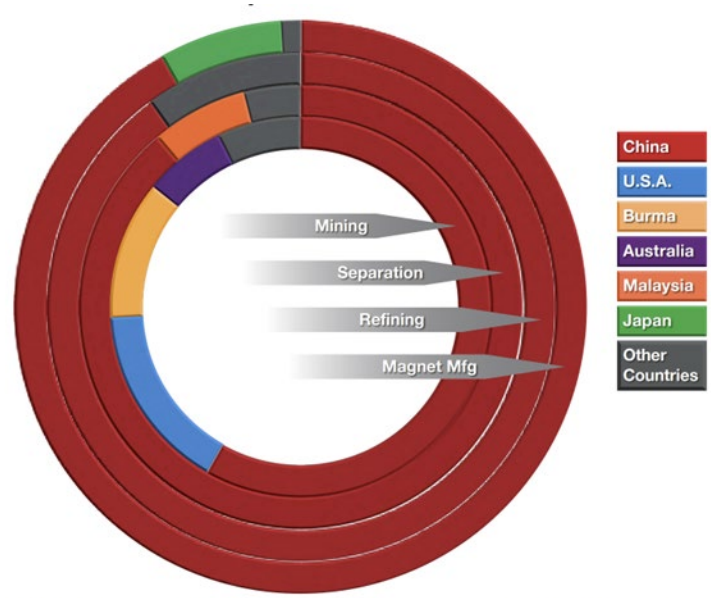

Figure 5: Geographical concentration of supply chain stages for sintered NdFeB magnets, 2019[28]

A number of initiatives to return rare earth element extraction and processing to the U.S. are in effect, such as the reopening of the Mountain Pass Mine in California by MP Materials. The Mountain Pass Mine is expected to begin operations with a high priority on the separation and refinement of bastnasite ore to produce high-purity neodymium-oxide. The refined rare earth oxide will be sent to nearby facilities within the country for the production of NeFeB magnets[29], [32]. Efforts are also being directed toward development of a new mining facility for rare earths in Bear Lodge Wyoming.

The search for a stable supply of rare earths has led to the investigation of their recovery from various types of waste. These wastes include but are not limited to tailings, electronics, batteries, magnets, hydrometallurgy residues, polishing powders, and rare earth catalysts[29], [33], [34]. However, due to the similar physical and chemical properties of rare earths significant challenges remain to be overcome in extracting individual rare earths in a cost-effective and eco-friendly manner.

The rare earths consist of the seventeen elements, highlighted in Figure 6. The fifteen known as the lanthanides are in the f-block row, ranging from lanthanum to lutetium and have similar atomic masses. Scandium and yttrium are not in the f-block series but are considered rare earths because their properties are similar to the lanthanides. Selected properties of the REEs are given in Table 4. The rare earths are often categorized as “light” or “heavy” divisions where light rare earths (LREE, atomic #’s 57-63 & 21) include lanthanum through europium plus scandium. The heavy rare earths (HREE, atomic #’s 64-71 & 39) range from gadolinium to lutetium plus yttrium.

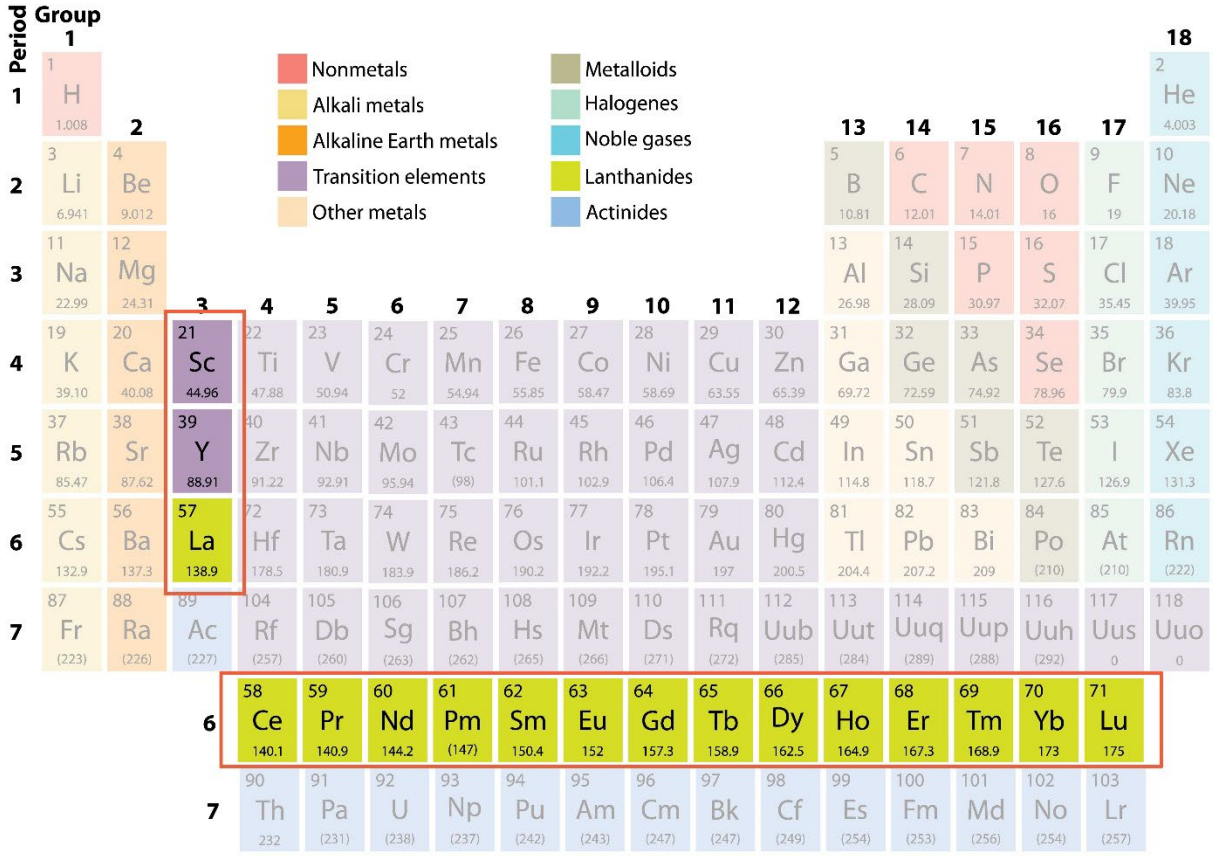

Figure 6: Periodic Table of elements. The lanthanides are highlighted in yellow and yttrium and scandium are highlighted in purple[35].

	REE	Atomic No.	Atomic Weight (g/mol)	Melting Point (°C)	Boiling Point (°C)	Ionic Charge (+)	Ionic Radius (nm)
Light	Scandium	21	44.956	1541	2836	3	---
	Lanthanum	57	138.906	918	3457	3	0.103
	Cerium	58	140.115	798	3426	3	0.102
	Praseodymium	59	140.908	931	3512	3	0.099
	Neodymium	60	144.240	1021	3068	3	0.098
	Promethium	61	145.000	1042	3000	3	0.097
	Samarium	62	150.360	1074	1791	3	0.096
	Europium	63	151.965	822	1597	3	0.095
Heavy	Gadolinium	64	157.250	1313	3266	3	0.094
	Terbium	65	158.925	1356	3223	3	0.092
	Dysprosium	66	162.500	1412	2562	3	0.091
	Holmium	67	164.930	1474	2695	3	0.090
	Erbium	68	167.260	1529	2863	3	0.089
	Thulium	69	168.934	1545	1947	3	0.088
	Ytterbium	70	173.040	819	1194	3	0.087
	Lutetium	71	174.967	1663	3395	3	0.086
	Yttrium	39	88.906	1522	3203	3	---

Table 4: Rare earth elements and some selected properties[11], [36].

The principle rare earth minerals include monazite, a phosphate-based mineral ($REPO_4$) and bastnasite a carbonate mineral ($RECO_3$), These minerals contain a high enough rare earth concentration to make it economically feasible to mine and process[29], [37]. Monazite typically contains 60-62 weight percent (wt%) rare earth oxide (REO) with varying compositions of La, Y, and Ce. Bastnasite can contain 65-75 wt% REO composed of Ce, La, Y, and Nd.

1.5. Background on rare earth extraction

Since rare earths have similar chemical properties, their separation from each other is challenging. Rare earths are extracted using either a hydrometallurgical or pyrometallurgical method, each with various advantages and disadvantages. Rare earth hydrometallurgy involves

the leaching of rare earths with an acidic solution and includes solvent extraction, ion exchange and precipitation to concentrate and purify the solution [34]. While the leaching process is simple, it involves multiple steps, each generating its own waste stream that requires treatment.

Compounding the issue of REE separation is the fact that REE-bearing mineral deposits are unique and an exclusive process for their extraction and refinement must be developed. Process development for a REE mine is substantially more costly in time and money than other mining opportunities. Figure 7 presents the mineral-processing flow for Mountain Pass mine, for one type of ore.

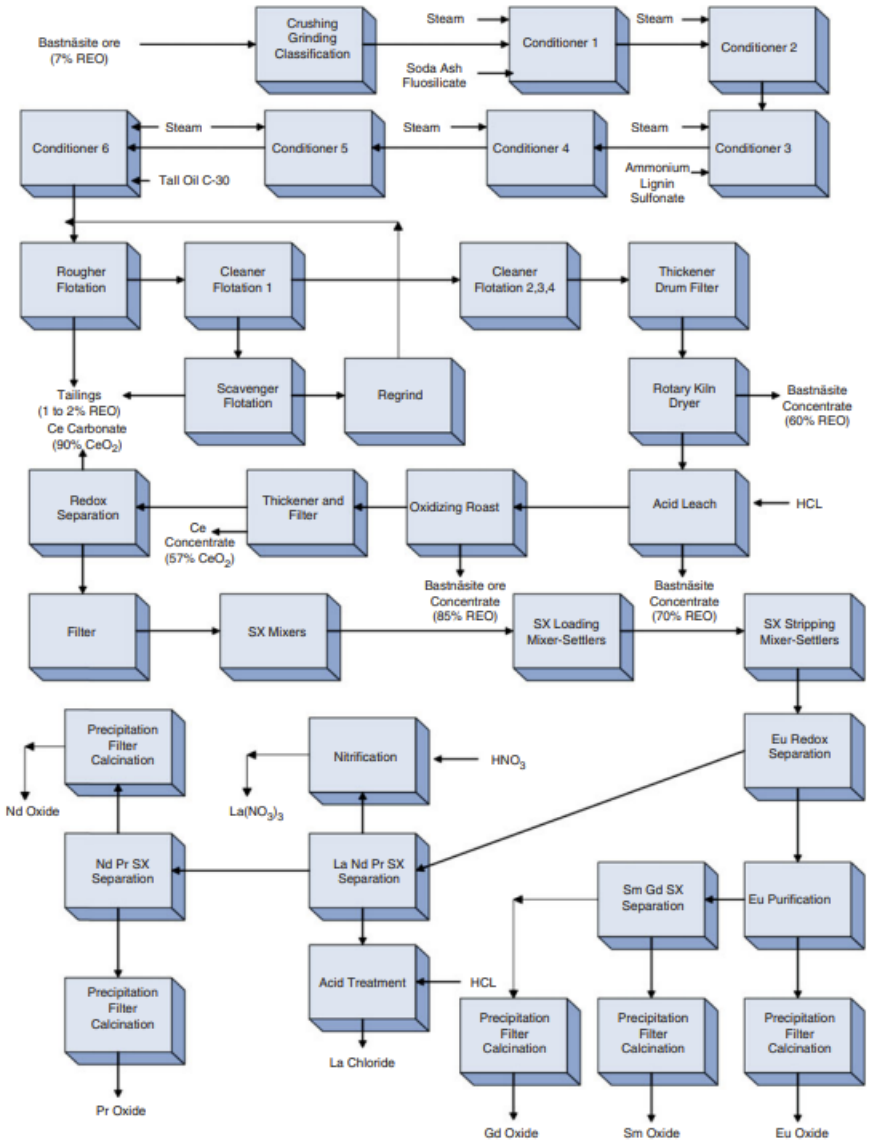

Figure 7: Rare earth mineral-processing flow sheet for the Mountain Pass mine [6]

Rare earth pyrometallurgy uses heat and additives to induce high temperature chemical reactions in a REE-containing feedstock in order to concentrate the desired REEs. The results of the process are gaseous, liquid, and/or solid products high in REE concentration. The cost to meet high energy requirements, heavy corrosion of equipment, and generation of waste dust and gases are the main disadvantages to the pyrometallurgical method. The extraction of REEs from

minerals is complicated by the fact that rare earth ore constituents can differ to the point that a standard process for their extraction isn't feasible, thus compounding the issue of rare earth processing and recovery.

1.6. REE ore chlorination

Chlorination of REO converts the oxides into rare earth chlorides (RECl) that can be dissolved in an aqueous solution for the refining of REEs. The amenability of the REOs to chlorination roasting following by water leaching presents an attractive opportunity to extract rare earths using MNPs. Much work has been done concerning rare earth chlorination and a host of chlorinating agents have been used, including hydrogen chloride, carbon, and chlorine ("carbochlorination"), chlorine, and ammonium chloride [35]. The purpose of the chlorinating roast is to convert the contained REEs to water- or acid-soluble products. Of the earliest papers, Meyer et al., noted one of the primary difficulties of converting REO to RECl is avoiding the formation of insoluble rare earth oxychlorides [38].

Previous research done at Montana Tech by Gaede[39] explored the viability of a pyrometallurgical chlorination process to convert REOs to RECls. Initial experiments were conducted using surrogate samples with only REOs followed by experimentation with actual rare earth ores and concentrates. The conversion process results in insoluble oxides of most of the gangue elements (low commercial value elements or metals) and soluble RECls. Gaede reported that the optimal parameters for rare earth oxide to chloride conversion were a 21:1 molar ratio of ammonium chloride to concentrate, and a 1-hour roasting duration at a temperature of 330^{o}C. Experiments performed under these conditions resulted in overall conversion efficiencies of 94.5% for rare earth bearing ore and 92.2% for the rare earth concentrate samples[40]. The dissolved rare earths could theoretically be separated and isolated using vapor phase extraction

and condensation or alternatively leached to solubilize the REEs in preparation for hydrometallurgical solution purification and separation operations. Additional results by Gaede showed that the chlorination method is sufficiently robust and flexible to operate effectively within relatively large windows of process parameters while still achieving over 90% conversion. His work showed the potential for this technique to eliminate processing steps for rare earth extraction such as beneficiation, complex leaching, and recirculation/regrind steps and to develop an improved industrial process.

A drawback of the chlorination process is the chlorination of gangue constituents that follow with the rare earth chlorides. These waste elements primarily include calcium and iron chlorides that complicate rare earth purification. An improved method of separating dissolved rare earth chlorides from the gangue elements would be beneficial.

1.7. Thesis statement

The selectivity of magnetite nanoparticles (MNPs) adsorption for various elements in aqueous solutions was investigated. Elements were selected on a basis of environmental concern and/or economic value. The goal of this study was to determine the effects of coexisting ions and other parameters on selective element extraction using MNPs. Preliminary research was done with surrogate solutions of cobalt, copper, chromium, lanthanum, and cadmium. Subsequent work focused on rare earth element solutions and investigating their potential for selective extraction. Finally, experiments for the selective extraction of rare earths from gangue elements (Fe and Ca) from the product of rare earth ore concentrate chlorination were conducted. It is hypothesized that by controlling parameters such as pH and MNP dosage, the selectivity of magnetite for certain elements can be exploited.

2. Experimental procedures and Methods

2.1. Materials

Commercially available magnetite (Fe_3O) was purchased from SkySpring Nanomaterials (Fe_3O_4, 98+%, 20-30 nm) and these MNPs served as the metal ion adsorbent for all experiments described in this work. Inductively coupled plasma ICP standards were purchased from Inorganic Ventures and Sigma-Aldrich. The surrogate solutions were prepared using chemicals, listed below with their respective purities, purchased from Fisher Scientific.

- Chromium(III) sulfate hydrate ≥95% purity.
- Cadmium sulfate octahydrate ≥98% purity
- Cobalt(II) sulfate heptahydrate ≥98% purity
- Lanthanum(III) sulfate hydrate ≥99.9% purity
- Ytterbium(III) sulfate octahydrate, 99.9% (REO)
- Gadolinium(III) sulfate octahydrate, 99.9% (REO)
- Samarium(III) sulfate octahydrate, 99.9% (REO)
- Neodymium(III) sulfate octahydrate, 99.9% (REO)
- Praseodymium(III) sulfate octahydrate, 99.9% (REO)
- Dysprosium(III) chloride hydrate, 99.9% (REO)
- Zinc sulfate heptahydrate, 99.5%
- Manganese(II) sulfate tetrahydrate, 99%
- Aluminium sulfate octadecahydrate, 98%

- Iron(II) sulfate heptahydrate, ACS, 99+%
- Iron(III) sulfate pentahydrate, 97%,
- Scandium(III) sulfate hydrate, 99.9% (REO)
- Strontium chloride, 99.99%
- Terbium(III) chloride hexahydrate, 99.99% (REO)
- Yttrium(III) chloride hexahydrate, 99.9%
- Erbium(III) chloride hydrate, 99.9% (REO)
- Scandium(III) chloride hexahydrate, 99.9% (REO)
- Thulium(III) chloride hydrate, 99.9% (REO)
- Calcium chloride, dried, powder, 97%

2.2. Single- and multi-element loading experiments

All metals evaluated in this study for competitive behavior of adsorption onto magnetite were individually evaluated as single-element solutions in preparation for subsequent experiments using multi-element solutions. Duplicates were run for each sample in an experiment. Stock surrogate solutions were prepared by dissolving either chloride or sulfide-based compounds containing the desired element and in 18 MΩ DI water. The experiment conditions were based off previous MNPs research with copper and used as a starting point for further experiments. Adsorption experiments were conducted with 3.5 g of MNPs and mixed with 250 mL of surrogate solution at a starting concentration of 100 ppm of each metal for 1-hour at the intrinsic pH and temperature using an agitation speed of 150 rpm. MNPs were wetted with methanol before being added to the surrogate solution. The standard dose of MNPs and

metal ion solution were the same for each experiment unless stated otherwise. At the end of the set contact time, the MNPs were removed, and the solution was filtered. Approximately 20 mL of remaining solution was stored in a separate container at a pH below 2 for future ICP analysis.

The loading capacity and adsorption efficiency % were calculated using equations 3) and 4):

$$q = \frac{(C_0 - C_e)V}{m} \quad 3)$$

where q is the loading capacity (mg/g), C_0 and C_e are the initial and final concentrations (mg/L), respectively, V is the total volume of the solution (L), and m is the mass of the adsorbent (g). Loading capacity quantifies metal ion removal from solution per gram of adsorbent. The adsorption efficiency is given by Equation 4).

$$Adsorption\ Efficiency\ \% = \frac{(C_0 - C_e)}{C_0} * 100 \quad 4)$$

where C_0 and C_e are defined in the same manner as in Equation 3). Adsorption efficiency expresses the percentage of metal ions recovered from solution by comparing the initial and final metal ion concentrations.

2.3. Scoping experiment series

Loading capacity experiments were performed to determine MNPs ability to adsorb the following ionic species/elements: Cu(II), Cr(III), La(III), Co(II), and Cd(II). Both single and multi-element surrogate solutions were prepared with initial concentrations of approximately 100 ppm for each element except Cr(III) which had an initial concentration of ~65 ppm. Experiments were performed in duplicates for each sample. Once reference values for loading capacity and removal efficiency were established for the individual elements, the multi-element experiments

were performed at the same ion concentration (using the same stock solution) and MNP dosage. Single element experiment equilibrium pH values are listed in Appendix A: Table 18. Multi-element experiment equilibrium pH values are listed in Appendix A: Table 19.

2.4. Rare earth experiment series

Further magnetite adsorption experiments were designed with an expanded list of rare earths. Nine rare earth elements (Sc, Y, La, Gd, Dy, Tb, Er, Tm, Yb) were selected for evaluation over a diverse range of ionic radius and were investigated for magnetite uptake capability and selectivity. Except where stated otherwise, the solution pH was not adjusted prior to or during the experiment. All solutions were prepared by dissolving chloride salts of each element to create 100 ppm concentrations. A dosage of 3.5 g MNP was added to 250 mL of surrogate solution and stirred at 150 rpm for 1-hr. Single element experiment equilibrium pH values are listed in Appendix A: Table 18. Multi-element experiment equilibrium pH values are listed in Appendix A: Table 19.

2.5. REE ore experiment series

Single element surrogate solutions of approximately 100 ppm and 1000 ppm were prepared from chloride-based compounds for the REE (Ce, La, Gd, Dy) and gangue elements (Fe(II) and Ca). The pH of each solution was not adjusted and 3.5 g of MNP was added to solution and mixed for 1-hour before removal. High and low ion concentrations were used to determine how ion concentration affected loading capacity. Iron was omitted from the 1,000 ppm experiments because the projected concentration values in the leach liquor range from 20,000 ppm and above.

A leach liquor stock was prepared by dissolving approximately 30 g of chlorinated REE ore concentrate (calcine) in 500 mL of 18 MΩ DI water. For the experiments defined in Table 16, the pH was left at its intrinsic value and the iron was not precipitated and filtered out of

solution. A smaller total volume of 12.5 mL was used because of the limited quantity of leach concentrate solution available for the experiments. In the experiments delineated in Table 17, REE ore leach liquor was diluted by one-quarter (25%) of its original concentration. The pH was adjusted to 4.43 and the precipitated iron was filtered from the solution. The same proportions of 250 mL and 3.5 g of MNPs were used but scaled down to 6.25 mL and 0.0875 g.

2.6. Kinetics

Kinetics experiments were performed to determine the adsorption rate of contaminants onto the MNPs. Experiments were conducted using a known starting metal ion concentration and a dose of 10.5 g MNPs in 750 mL of 18 MΩ deionized (DI) water, agitated at 600 rpm. The metal ion concentration and pH were recorded by taking samples throughout the course of 3-hours. All experiments were conducted at intrinsic pH and room temperature. All samples were analyzed by ICP.

2.7. REE ore chlorination

The chlorination roast was conducted by Katie Schumacher using the following procedure: an alumina reaction vessel was placed within the Thermcraft rotary furnace's (Model# TRT-3-0-24-ICJ13295/ 1A) three-inch Inconel tube. A 21:1 ratio of ammonium chloride to rare earth oxide provided the requisite excess of ammonium chloride for the reaction. After accounting for unreactive material within the rare earth concentrate, a molar ratio of three parts ammonium chloride to one-part rare earth concentrate was used. A blended charge of 20 grams of concentrate and 60 grams of ammonium chloride was added to the alumina reactor vessel. The rare earth ore concentrate and ammonium chloride were held in the hot zone of the furnace within an alumina reactor vessel with rod that ran the length of the Inconel tube. The Inconel tube rotated at 20 revolutions per minute to facilitate mixing throughout the roasting

process. Argon gas flowed through the apparatus at 500 milliliters/min to remove the gaseous reaction products, NH_3 and H_2O. The outlet gases counter-current flowed through a packed absorption column manufactured by Büchiglasuster. The furnace was ramped to 360 ºC at 4 degrees a minute, equating to an internal reactor vessel temperature of 340 °C, and held at temperature for 90 minutes. A depiction of the experimental setup is shown in Figure 8.

Figure 8: The Thermcraft instrument is located on the left side of the picture and the Buchiglas scrubber on the right.

After the furnace cooled, the chlorinated rare earth concentrate was removed from the furnace. The chlorinated rare earth concentrate was mixed with 18 megaohm water to dissolve the rare earth chlorides. Iron and calcium are gangue elements leftover from the roasting process.

Lanthanum, dysprosium, cerium, and gadolinium are the highest concentration rare earths. A partial elemental analysis of the REE ore concentrate is displayed in Table 5.

Table 5: Partial elemental analysis (wt%) of domestic source ore concentrate. Only the elements that were later measured in the surrogate studies are shown.

RE ore concentrate	
Element	wt%
Ca	3.65
Ce	10.5
Dy	0.26
Fe	18.9
Gd	0.33
La	9.63

2.8. ICP Analysis

An iCAP 6500 Series inductively coupled plasma-optical emission spectrometry (ICP-OES) was used to analyze each solution sample. All ICP samples were prepared by diluting the sample to the desired concentration with 5% nitric acid. Samples were diluted to within ICP concentration limits of a maximum of 20 ppm. A three-point calibration curve was established before each ICP test. A 10 ppm standard and 5% nitric blank were analyzed every 10 samples to

monitor instrument drift. The emission wavelengths of all elements used for ICP analysis are shown in Table 6.

Table 6: Elements and respective emission wavelengths used for ICP analysis.

ICP Analysis	
Element	**Wavelength(nm)**
Al	**396.1**
Ca	**393.4**
Sc	**361.4**
Cr	**267.7**
Mn	**257.6**
Fe	**259.9**
Co	**228.6**
Cu	**324.7**
Zn	**213.8**
Sr	**407.7**
Y	**371**
Cd	**226.5**
La	**379.4**
Ce	**448**
Eu	**381.9**
Gd	**336**
Tb	**350.9**
Dy	**400**
Er	**337.3**
Tm	**346.2**
Yb	**328.9**

3. Results and discussion

3.1. Scoping experiments

Preliminary experiments were performed to examine the relative selectivity of magnetite for several different ionic species. Thirteen elements were chosen based on the criteria of economic value, toxicity, and valence state (+2 vs +3 charge). Experiments were designed to evaluate each element individually to provide a baseline for comparison with its adsorption characteristics in subsequent experiments conducted on multiple-element solutions. Scoping experiments were divided into three subsections based on the surrogate solution mixture of the selected elements. Single element experiment equilibrium pH values are listed in Appendix A: Table 18. Multi-element experiment equilibrium pH values are listed in Appendix A: Table 19.

3.1.1. Scoping Experiments (Series_1)

Loading capacity experiments were performed to determine MNPs ability to adsorb the following ionic species/elements: Cu(II), Cr(III), La(III), Co(II), and Cd(II). Both single and multi-element surrogate solutions were prepared with initial concentrations of approximately 100 ppm for each element except Cr(III) which had a beginning concentration of ~65 ppm due to partially hydrated chromium salts. Once reference values for loading capacity and removal efficiency were established for each element multi-element experiments were performed at the same ion concentration and MNP dosage. A kinetics experiment was performed using the above-mentioned elements to measure the time required for adsorption to reach equilibrium in the multi-element solution. The multi-species experiments examined changes in loading capacity and removal efficiency to determine if selectivity occurred between the given species. Additional experiments were performed where variable parameters such as pH or MNP dosage were

individually altered to evaluate selectivity. Unless stated otherwise, all experiments are standardized to use 250 mL of surrogate solution mixed with 3.5 g of MNPs for a duration of 1-hour at the natural pH of the solution.

Figure 9 shows the single and multi-element results for adsorption onto MNPs under different pH conditions. The pH of the single element experiments and the experiment labelled "3.36 pH" were left at their intrinsic pH value. Four multi-element experiments were performed in which the solution pH was adjusted from the intrinsic pH value of 3.36. In one multi-element experiment, the starting pH was adjusted to 4.43 and allowed to naturally change over the experiment duration. In the other three experiments, pH was adjusted to 2.5, 3.31, and 4.5, respectively, and held constant at those values for the duration of the experiments by the addition of sulfuric acid.

The results of all experiments revealed that the adsorption efficiency of Cr(III) was high in comparison to the other elements in all experiments; 98% or higher adsorption efficiency was realized in single and competitive environments in most circumstances. These results indicate a competitive advantage for preferential Cr(III) uptake at the intrinsic pH 3.36. Adjustment of the intrinsic pH of the solution to 4.43 caused a significant increase in adsorption efficiency for La(III) and Cu(II). The pH change improved adsorption efficiencies of La(III) from 58% to 98% and Cu(II) from 47% to 92%. Elevating the starting pH to 4.43 yielded adsorption efficiency values similar to lanthanum's single element condition. The experiment yielding the lowest adsorption values for Cr(III) occurred when adjusting the pH to 2.5 and maintaining it for the duration of the experiment which resulted in a adsorption efficiency of approximately 20%.

Overall, these results demonstrate capability to attain high adsorption efficiencies of all elements surveyed except for Co(II), which had the lowest performance at a 47% adsorption in a

single element solution and also exhibited the lowest adsorption efficiency in the multi-element solution experiments. Lowering the pH to increasingly acidic conditions hinders the adsorption of all elements and suggests that Cr(III) could be selectively adsorbed then stripped by adjusting the pH.

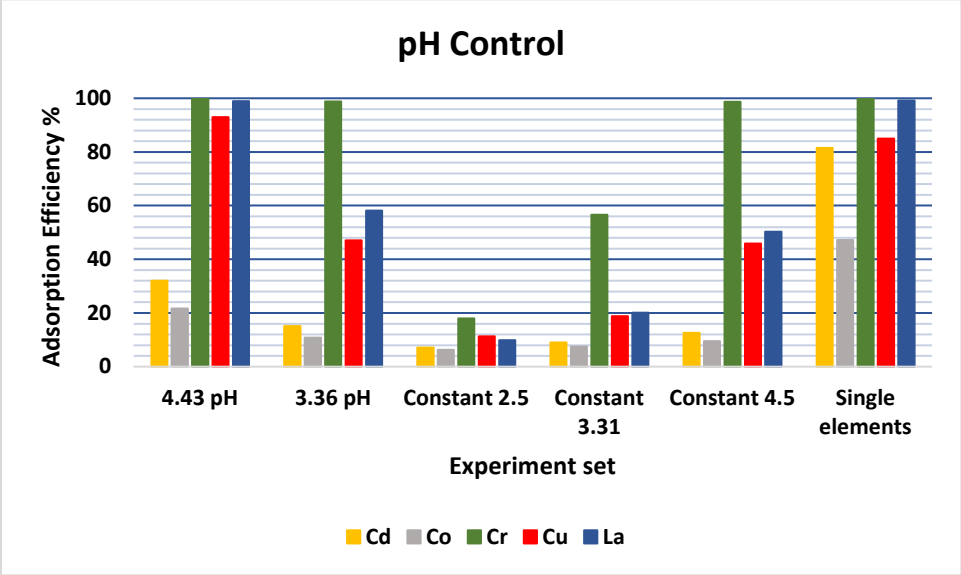

Figure 9: The effect of pH on the adsorption of multiple element solutions obtained by magnetite nanoparticles and single element test results. (Experimental conditions $C_{element}$ = ~100 ppm, MNP = 3.5 g, V = 250 mL)

Figure 10 displays the results of the kinetic experiments conducted to examine the rate of adsorption of the mixed elements onto MNPs and to determine whether equilibrium was reached within the 1-hour timeframe of the single and multi-element experiments. The experiment was performed over a 3-hour period; the experimental parameters included mixing 450 mL of multi-element solution with 6.3 g of MNPs and each initial element concentration was approximately 100 ppm, except for Cr(III) at ~65 ppm and La(III) at ~73 ppm. The pH of the solution was not adjusted and started at ~3.3.

The greatest rate of adsorption in the beginning of the experiment was displayed by Cr(III), ~77% of its initial concentration adsorbed by magnetite within the first minute. Cr(III)

also maintained the highest value of adsorption efficiency, (99%). at the end of the experiment. The maximum adsorption rates for all elements surveyed occurred within the first minute of the experiment and magnetite saturation was achieved within the first 10 minutes for all elements as sites became occupied, verifying that 1-hour mixing conditions would suffice for all subsequent experiments. Additional data located in Appendix A: Figure 27.

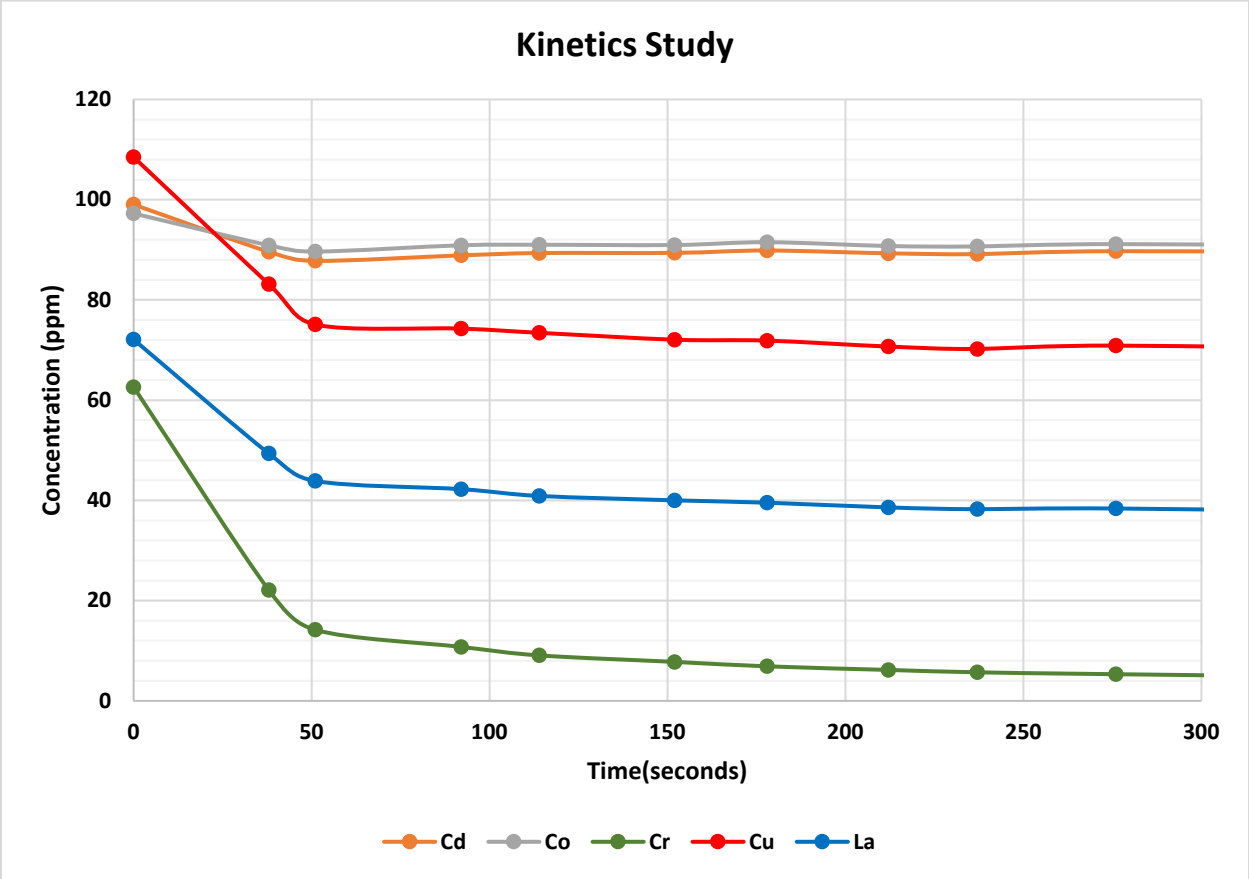

Figure 10: Change in concentration vs time for 450 mL of mixed surrogate solution mixed with 6.3 g of magnetite for 3 hours.

MNP dosage was varied to determine the effects of it on loading capacity and selectivity shown in Figure 11. The MNP dosage was varied by three different fractions of the standard 3.5g

value used in previous experiments. The MNPs were added to 250 mL of surrogate solution containing approximately 100 ppm of each element and ~65 ppm of Cr(III) and agitated for 1 hour. Results from previous single element and multi-element experiments are included in the figure to facilitate comparison.

Chromium(III) adsorption efficiency exhibited higher values than the other elements though MNP dosage was lowered to one-third of its original dosage and displayed adsorption efficiency values above 80% while the next highest was Cu(II) at 22% with 1.17 g of MNPs. As the MNP dosage increased, the adsorption efficiencies of the other elements improved as the chromium adsorption efficiency approached 100%. The adsorption values increased for all elements as MNP dosage was raised. Another trend observed is that the uptake order of La(III) ions over Cu(II) weakens and seems to reverse as MNPs dosage is decreased even though the selectivity suggests preference for a higher valence element.

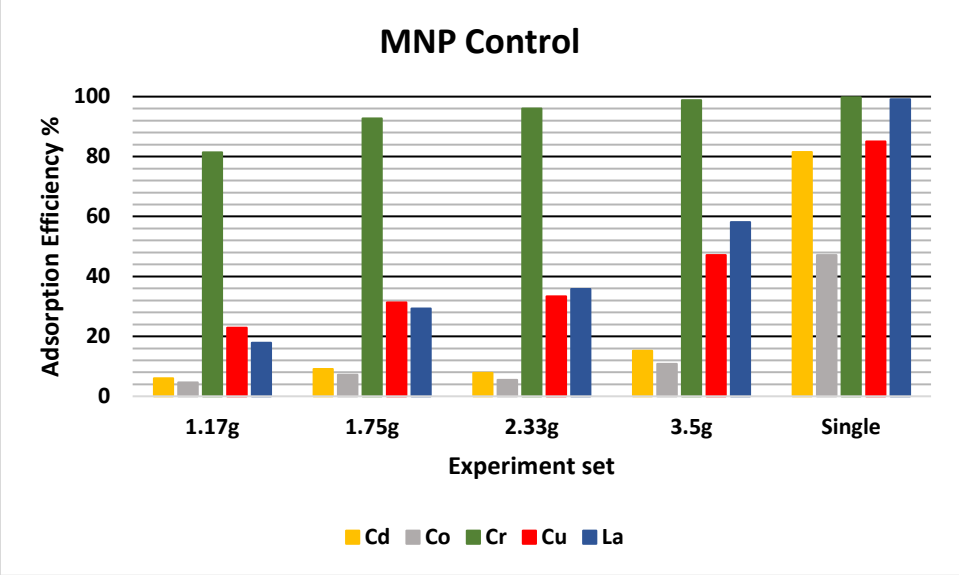

Figure 11: The effect of MNP dosage on the adsorption of multiple element solutions obtained by MNPs and single element test results. (Experimental conditions $C_{element}$ = ~100 ppm, MNP = 1.17, 1.75, 2.33, or 3.5 g, V = 250 mL)

Figure 12 reports the loading capacity values, expressed as q (mmol/g MNPs) calculated from equation 3, using the results of Figure 11. As the MNP dosage decreases, the loading capacity of Cr(III) increases from 0.0874 mmol/g to 0.217, a value exceeding its single element performance. Lanthanum (III) follows a different loading capacity trend, decreasing as MNP dosage is lowered but appearing to reach a constant value of ~0.20 mmol/g though MNPs dosage continues to decrease. Cu(II), Cd(II), and Co(II) show an initial decrease in loading capacity values as MNP dosage is lowered from 3.5 g to 2.33 g but increases for 1.75 and 1.17 g MNP dosages. The element with the highest loading capacity does not always equate to high selectivity; rather, loading capacity and adsorption efficiency must be considered for evaluated selectivity.

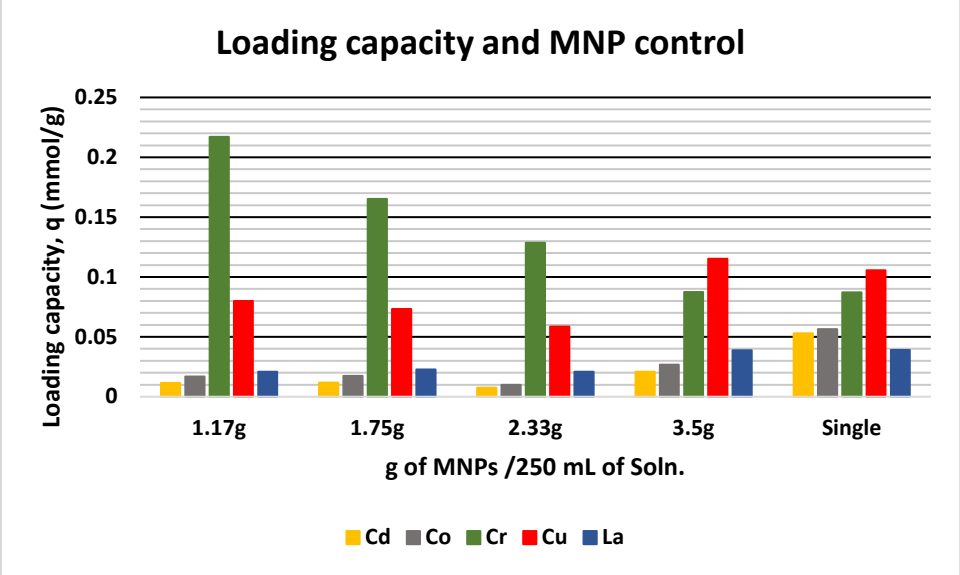

Figure 12: The effect of MNP dosage on the adsorption capacity of multiple element solutions obtained by MNPs and single element test results. (Experimental conditions $C_{element}$ = ~100 ppm, MNP = 1.17, 1.75, 2.33, or 3.5 g, V = 250 mL)

Adsorption efficiency and loading capacity results for Cr(III) from Figures 11 and 12 are plotted in Figure 13. Loading capacity and adsorption efficiency values are similar for the 3.5 g MNP dosage experiments in both single and multi-element environments (~99% in both circumstances), indicating high adsorption efficiency unique to Cr(III) when compared to the other surveyed elements. A high adsorption efficiency value (81%) for Cr(III) was obtained when using 1.17 g of MNPs (1/3 of the standard testing value). As loading capacity increases the adsorption efficiency decreases, suggesting that the max loading capacity of MNP does not occur with a 3.5 g dosage but at a dosage closer to 1.17 g for 250 mL of 65 ppm Cr(III) solution. Though further experimentation would be required, it seems plausible that it is possible to adsorb a majority of the Cr(III) ions by using multiple adsorption cycles with low MNP dosages.

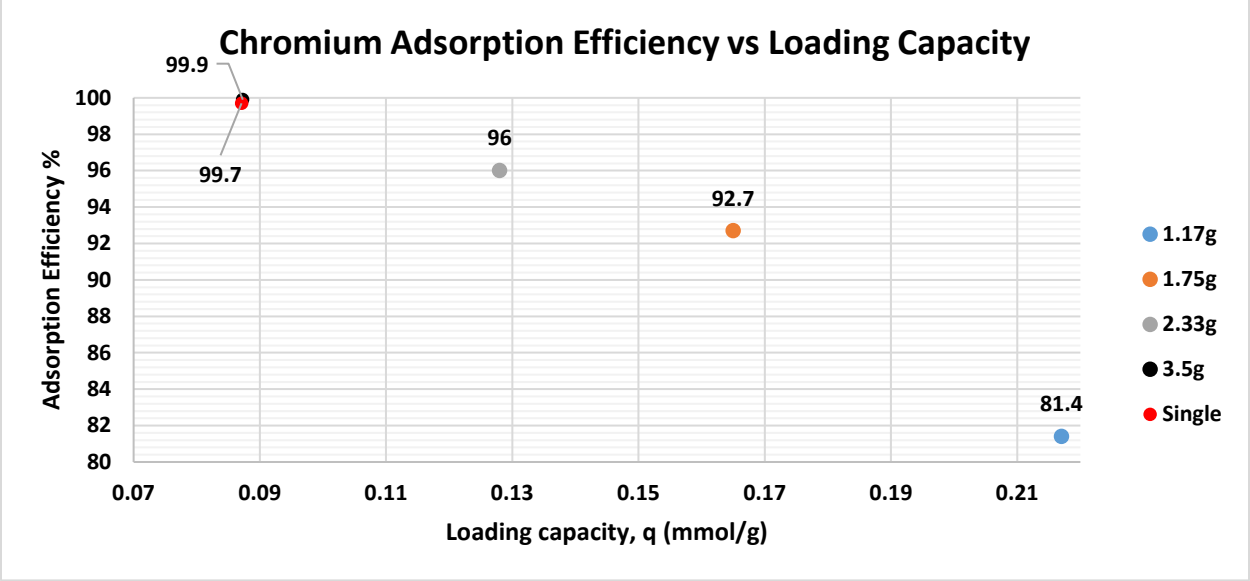

Figure 13: Chromium adsorption efficiency (%) plotted as a function of loading capacity at varying MNP dosages in single and multi-element solutions. (Experimental conditions $C_{element}$ = ~100 ppm, MNP = 3.5 g, V = 250 mL)

Table 7 contains K_d and $K_{Cr(III)/M}$ values calculated from data in Figure 9 using equations 3-) and 4-). K_d represents a mass-weighted partition coefficient between the liquid supernatant

phase and solid sorbent phase to help describe sorbent efficacy. K_d is a direct measurement of sorbent affinity for an analyte under the conditions in which it was measured. As this value increases, the sorbent material will be more likely to capture and hold the target species. A general rule is that values of 10^3 mL/g are considered good while values of or greater than 10^4 are considered outstanding. High selectivity coefficient values, $K_{Cr(III)/M}$, suggest that the MNPs will be more selective toward the target species while low values suggest competitive behavior between other species.

The calculated K_d and $K_{Cr(III)/M}$ values show that MNP affinity for Cr(III) is most prominent at a pH of ~4 and selectivity for Cr(III) is preferential over other elements. Adjusting the starting pH of the solution from 3.31 to 4.43 changes the K_d value for Cr(III) from 5,900 to 3,970,000 mL/g and the K_d value for La(III) from 99 to 6600 mL/g. While the MNPs will preferentially adsorb Cr(III) first, the high K_d values for La(III) and Cu(II) can be increased to values of 10^3 mL/g depending on pH, suggesting that MNP would be able to remove these elements given enough cycles after the majority of Cr(III) is removed. Cd(II) and Co(II) $K_{Cr(III)/M}$ values range highest for the given elements and suggests that they will hold no competitive advantage over the uptake of Cr(III) except when the pH is 2.5 and adsorbed species begin to strip. Based on these results, the suggested selectivity using MNPs is:

$$Cr(III) >> La(III) > Cu(II) >> Cd(II) > Co(II)$$

These results suggest that the selective removal of Cr(III) using MNPs is possible in solutions with other heavy metals (in +2 valence states) or rare earths.

Table 7: The Affinity of MNPs for Cr(III) and other coexisting ions in aqueous solution

Sample set	K_d, mL g^{-1}					$K_{Cr(III)/M}$			
	Cd(II)	Co(II)	Cr(III)	Cu(II)	La(III)	Cd(II)	Co(II)	Cu(II)	La(III)
pH 4.43	34	20	3970000	940	6600	117000	200000	4200	598
pH 3.36	13	9	5900	63	99	462	681	93	59
Constant pH 2.5	5	4	16	8	7	3	4	2	2
Constant pH 3.31	7	5	95	16	17	14	18	6	6
Constant pH 4.5	10	7	5900	62	74	575	796	95	79

3.1.2. Scoping Experiments (Series_2)

Experiments detailed in this section focused on examining the loading capacity and selectivity for additional rare earths (Gd and Yb) in single and multi-element conditions with La and Cr. Surrogate solutions of Gd(III), Cr(III), Yb(III), and La(III) were evaluated with various dosages of MNPs in order to determine the effects on selectivity and loading capacity. All experiments, unless stated otherwise, use 250 mL of the surrogate solution at intrinsic pH and were stirred for 1-hour using 3.5 g of MNPs.

Figure 14 shows the adsorption efficiency values of Cr(III), La(III), Gd(III), and Yb(III) with various MNP dosages (1.17, 1.75, 2.33, 3.5, and 7.0 g) and single element test results. Adsorption efficiency increased for all elements as MNP dosage increased but the change in adsorption efficiency was minimal for Cr(III) compared to the large average increase for the rare earth elements, which nearly doubled from 3.5 to 7.0 g of MNPs. In the single element adsorption experiments Cr(III) and La(III) displayed near complete adsorption while Yb and Gd displayed more modest levels of adsorption. Chromium (III) had the highest adsorption efficiency value for all experiments, a value of 96% in a multi-element environment while the rare earths averaged 35%. Ytterbium(III) and Gd(III) were similar in adsorption efficiency at each MNP dosage as well as in the single element tests. Lanthanum(III) had the lowest adsorption efficiency value from the multi-element solution but had a higher adsorption

efficiency than the other rare earth elements in the single-component solution, averaging 99% adsorption efficiency while Gb(III) and Yb(III) averaged 65% in the single element tests. Ytterbium(III) and Gd(III) adsorption efficiency values only exceed their single element tests during the 7.0 g of MNPs experiment in which both average ~88% adsorption. Selectivity for Cr(III) is achieved by controlling the MNP dosage because the adsorption efficiency of Cr(III) is significantly higher than the competing elements even at low MNP dosages.

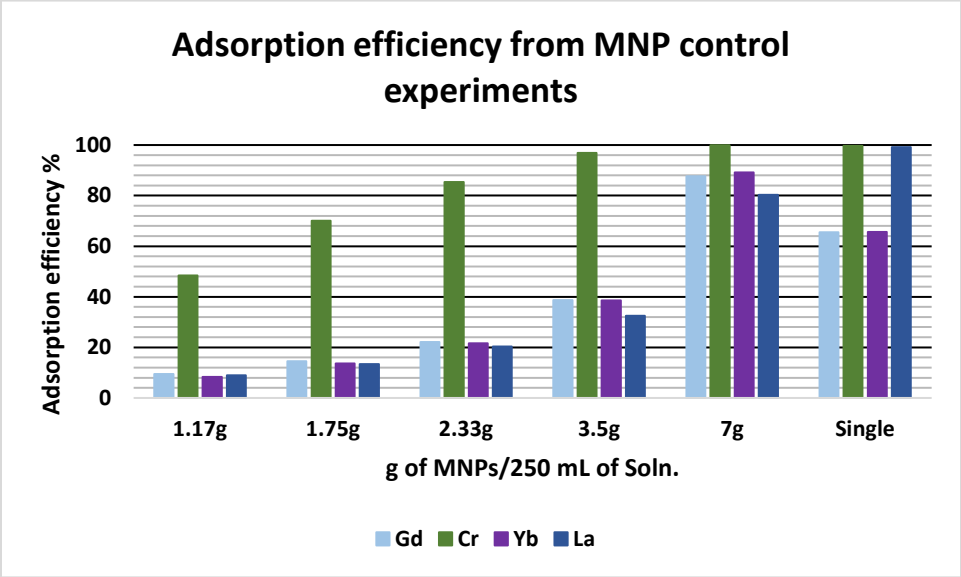

Figure 14: Effect of MNP addition on the adsorption of multiple element solutions obtained by MNPs and single element test results. (Experimental conditions $C_{element}$ = ~100 ppm, MNP = 1.17, 1.75, 2.33, 3.5 g, V = 250 mL)

Loading capacity values for the experiments of section 3.1.2 are displayed in Figure 15. The Cr(III) loading capacity value is lower in its single element experiment than the multi-element experiments because it is suspected that 3.5 g MNP dosage exceeds the minimum amount required for saturation. Rare earth elements La(III), Gb(III), and Yb(III), are closer to their maximum loading capacity in their single element experiments because these values continually decrease as MNP dosage decreases. The results disclosed in Figures 13 and 14

suggest the MNP adsorbent is selective for Cr(III) over multiple rare earth elements. Similar loading capacity and adsorption efficiency values between La(III), Yb(III), and Gd(III) do not indicate a competitive advantage of one rare earth over the other.

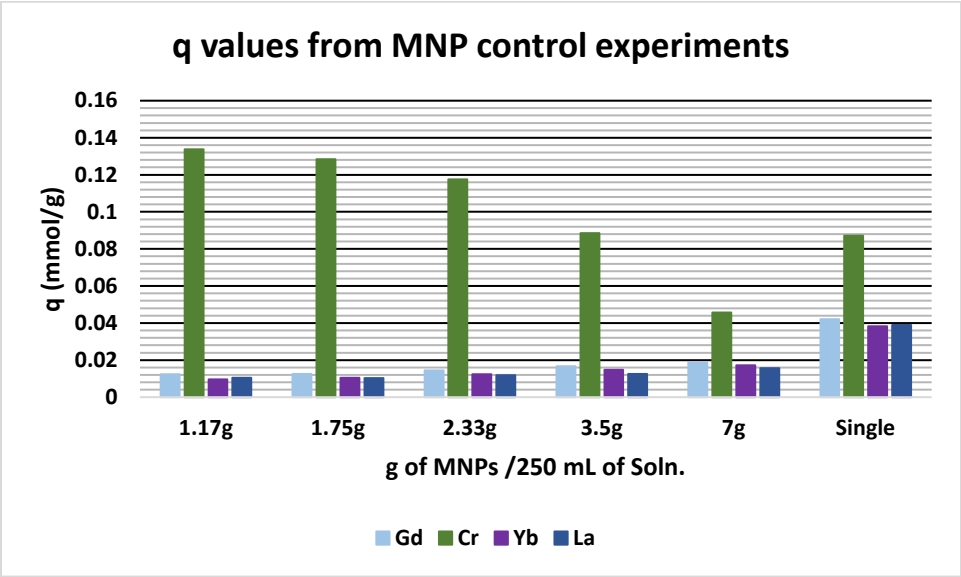

Figure 15: Effect of MNP addition on the loading capacity, q, of multiple element solutions obtained by MNPs and single element test results. (Experimental conditions $C_{element}$ = ~100 ppm, MNP = 1.17, 1.75, 2.33, 3.5 g, V = 250 mL)

3.1.3. Scoping Experiments (Series_3)

Scoping experiments focused on evaluating the established selectivity for Cr(III) in the presence of a wider range of elements including additional rare earths (Dy and Pr) and various gangue elements (Al, Mn, Fe, and Zn). The latter represent potential contaminants that are typically separated from the more valuable metals in an industrial process. Experiments were evaluated using a mixture of Cr(III), Gd(III), Yb(III), and La(III) as a base surrogate solution with one of the other six elements added (Fe(II), Mn(II), Al(III), Zn(II), for the gangue elements and Pr(III), Dy(III) for the rare earths). Each experiment involved 250 mL solution of ~100 ppm of each element at intrinsic pH mixed with 3.5 g of MNPs for 1 hour.

Figures 16 and 17 depict results from the same experiment. Results for the adsorption of Cr(III) and the rare earth and gangue elements are recorded in Figure 16. Of the six experiments, Cr(III) had an adsorption of 90% or above except when Al(III) was added to the mixture then the value was 73%.

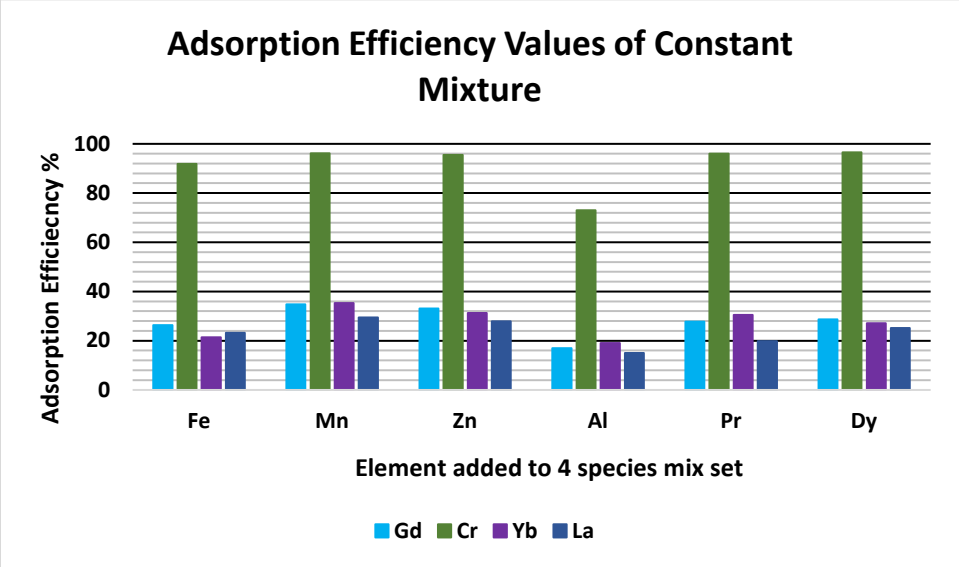

Figure 16: Effect of single element species on the adsorption of mixed species solution containing (Gd, Cr, Yb, La) by MNPs. Adsorption efficiency values are shown for the species only in the 4-element solution. (Experimental conditions $C_{element}$ = ~100 ppm, MNP = 3.5 g, V = 250 mL)

Adsorption efficiency values for the gangue elements and additional rare earths are shown in Figure 17. The elements with the three highest adsorption efficiency value in single tests are Pr(III), Fe(II), and Dy(III) with values of 97%, 84%, and 76%, respectively which demonstrates potential for the removal of these elements. The lowest adsorption efficiency value in a single and multi-element environment was Mn(II) with values of 32% and near 0% respectively.

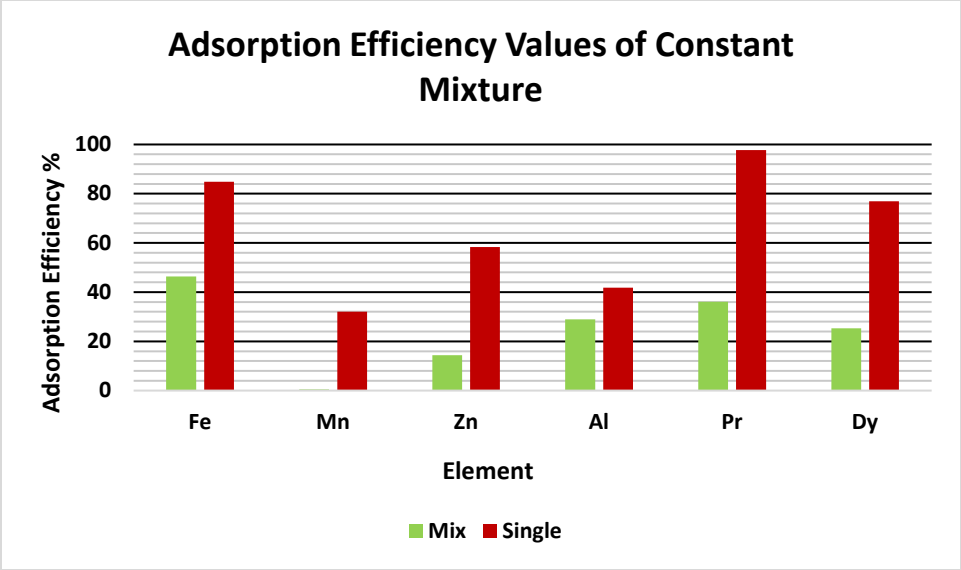

Figure 17: Effect of single element species on the adsorption of mixed species solution containing (Gd, Cr, Yb, La) by MNPs. Adsorption efficiency values are shown for the species added to the 4-element solution and their single element performance. (Experimental conditions $C_{element}$ = ~100 ppm, MNP = 3.5 g, V = 250 mL)

Figure 18 displays the loading capacity values, from experiments performed in Scoping Series_3, calculated using equation 3. The loading capacity values for Cr(III), displayed in Figure 18, averaged about 0.047 mmol /g MNPs except when paired with Al(III) then the measured loading capacity decreased to 0.037 mmol/g MNPs. In previous experiments, the loading capacity value was 0.087 mmol Cr(III)/g MNPs when Cr(III) competed against La(III), Cd(II), Co(II), and Cu(II) and 0.088 mmol/g MNPs when Cr(III) competed against Gd(III), Yb(III), and La(III), ,shown in Figures 13 and 15, respectively. Of the experiments performed to measure the loading capacity for Cr(III), those performed in Scoping Series_3 resulted in the lowest values of loading capacity when using 3.5 g of MNPs.

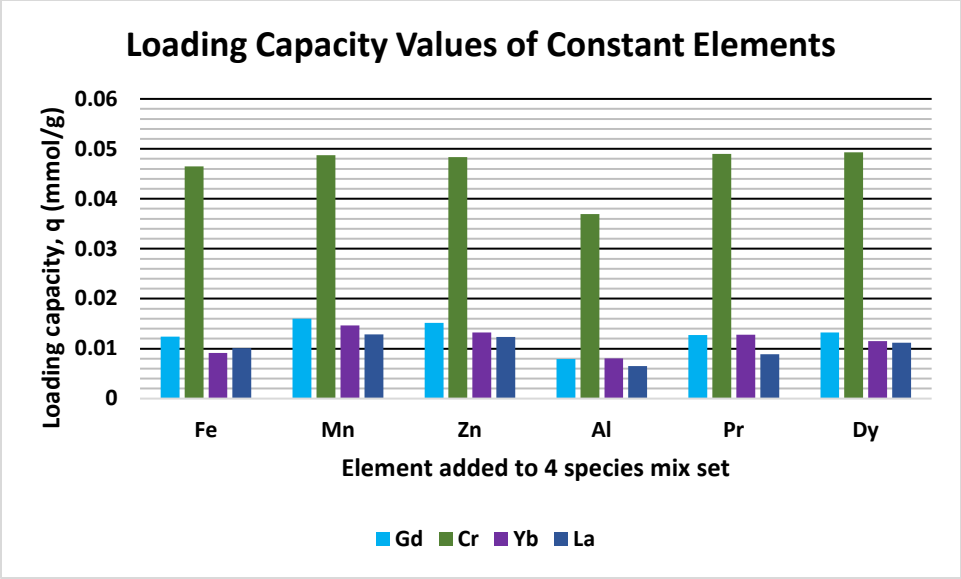

Figure 18: Effect of single element species on the adsorption of mixed species solution containing (Gd, Cr, Yb, La) by MNPs. Loading capacity values are shown for the species only in the 4-element solution. (Experimental conditions $C_{element}$ = ~100 ppm, MNP = 3.5 g, V = 250 mL)

Figure 19 represents the data of each of the six elements individually added to the 4-element mixture from Figure 18. Manganese (as Mn(II)) had the lowest loading capacity values in both single and multi-element environments with values of 0.025 and 0.0003 mmol/g MNPs, respectively. Aluminum (III) and Fe(II) had the next highest loading capacity values after Cr(III) for single and multi-element experiments. Praseodymium (III) had a slightly higher loading capacity value than Dy(III) in the single and multi-element experiments, 0.043 vs 0.040 mmol/g for single and 0.015 vs 0.012 for multi-element experiments. Gangue elements, Al(III) and Fe(II), are likely to be competitive over rare earth elements.

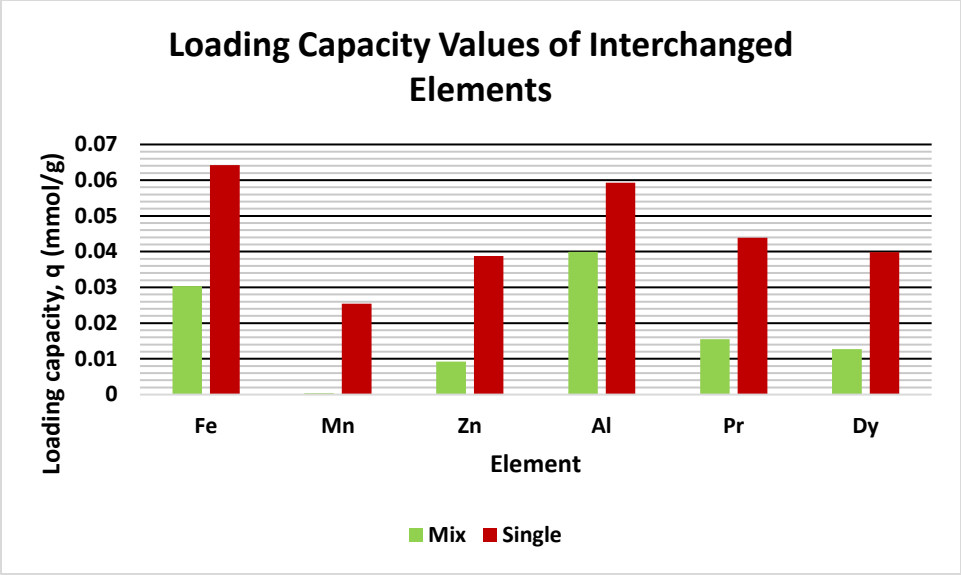

Figure 19: Effect of single element species on the loading capacity of mixed species solution containing (Gd, Cr, Yb, La) by MNPs. Loading capacity values are shown for the species only in the 4-element solution. (Experimental conditions $C_{element}$ = ~100 ppm, MNP = 3.5 g, V = 250 mL)

Table 8 represents the K_d and selectivity coefficient values for the elements chosen for the Series_3 experiments. The column marked "X" represents one of the six additional elements (Fe, Al, Mn, Zn) added to the base 4-element mixture (La, Cr, Gd, Yb) and which subsequent dataset is shown. Across all experiments Cr(III) yielded favorable K_d values for selectivity of approximately 10^3 in most cases. Only when competing with Fe(II) and Al(III) did the K_d value for Cr(III) drop below 'good' values with 193 mL/g being the lowest when competing with Al(III). All other elements consistently yield low K_d values, not exceeding 40. For $K_{Cr(III)/M}$ values, the highest was 5800 for Mn(II), indicating that MNP has a low affinity for this species.

Table 8: MNP affinity for Cr(III) and other coexisting ions in aqueous solution. X represents the element (Fe, Al, Mn, Zn) that was added to the 4-species solution (Cr, Gd, La, Yb) in each experiment.

	Sample set	K_d, mL g^{-1}					$K_{Cr(III)/M}$			
Element added to 4-species solution (X)		Gd	Cr	Yb	La	X	Gd	Yb	La	X
	Fe	26	802	19	22	62	31	41	37	13
	Mn	38	1800	39	30	0.31	47	45	60	5800
	Zn	35	1500	32	28	12	43	46	54	125
	Al	15	193	16	13	29	13	11	15	7
	Pr	27	1700	31	18	40	63	56	98	43
	Dy	29	2000	26	24	24	69	75	83	82

3.2. Rare earth experiments

The results from the scoping experiments discussed in Section 3.1 assisted in designing subsequent experiments because they showed that MNPs can adsorb a multitude of heavy metals and rare earth elements. Of particular interest is the ability of MNPs to capture rare earth elements because of the importance of these elements in a wide variety of technologies, and the difficulty in separating them. Further, MNP adsorption experiments were designed with an expanded list of rare earths. Nine REEs (Sc, Y, La, Gd, Dy, Tb, Er, Tm, Yb) were investigated for MNP uptake capability and selectivity. Except where stated otherwise, the pH of each solution was not adjusted. All solutions were prepared by dissolving chloride salts of each element to create 100 ppm concentrations to be mixed with the standard MNP dosage of 3.5 g. Single element experiment equilibrium pH values are listed in Appendix A: Table 18. Multi-element experiment equilibrium pH values are listed in Appendix A: Table 19.

The first experiments reported in Figure 20 involved rare earth elements (La, Yb, and Gd) examined in Section 3.1 (Series_2), and a rare earth not previously examined, scandium. These

rare earths were selected on the basis of their performance in previous experiments and cover the range of lanthanides.

For single element adsorption, ytterbium had the highest adsorption at 98% while scandium had the lowest at 43%; gadolinium and lanthanum adsorption efficiencies were 76% and 65%, respectively. For experiments performed in a multi-element environment at the intrinsic pH of 3.5, scandium had the highest adsorption efficiency at 59% while ytterbium had the lowest at 16% and gadolinium and lanthanum adsorption efficiencies were at 26% and 21%, respectively. In the single-element adsorption results, scandium had a moderately low adsorption efficiency value compared to the greater rare earth elements which may suggest that the lower mass rare earths perform worse than the higher mass rare earths. Adsorption efficiency results for lanthanum in the single-element experiments were low, averaging 65% whereas this value averaged about 98% when using lanthanum sulfate instead of chloride to prepare the solutions. The change in pH is most likely responsible for the difference because the sulfate-based solution had a pH of 3.6 on average where the chloride-based solution was around 5.16. When Sc, La, Yb, and Gb are mixed the trend of increasingly greater rare earth elements yielding higher adsorption efficiency values was not observed; instead, adsorption efficiency values varied from the lower to higher mass rare earth elements.

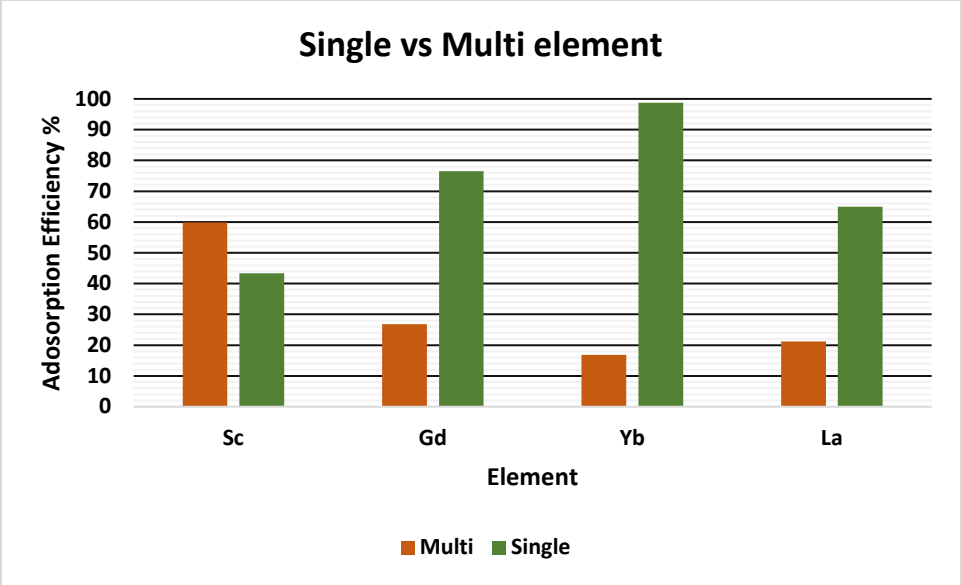

Figure 20: Data for the multi-element Gd, Sc, Yb, and La MNP adsorption and stripping studies in which 250mL of 100ppm solution was mixed with 3.5 g of MNPs for 1 hr at the natural pH=3.5

The results for the adsorption efficiency values of mixed and single element experiments using rare earth elements (Dy, Tb, Y, Sc, Er, and Tm) are reported in Figure 21. The purpose of these experiments was to evaluate MNP adsorption of scandium relative to a broader range of rare earths. Surrogate solutions were prepared using rare earth chloride salts to reach concentrations of approximately 100 ppm of each element and the standard dosage of 3.5 g of MNP was used for the adsorption experiments. The pH was varied to determine its effect on the adsorption of the mixed REE solutions, where the intrinsic pH of 4.05 was used in one experiment and then adjusted to 5.33 in another experiment.

For the single element experiments, represented by the green bars in the Figure 21, Sc and Y had the lowest adsorption efficiency values averaging about 44% while the other rare earths (Dy, Tb, Er, and Tm) had much higher adsorption efficiency values with an average of about 75%. The black bar represents adsorption efficiency values for each element from the multi-element experiments with an intrinsic pH of 4.05. Scandium had the highest adsorption

efficiency value averaging approximately 45% while the other rare earth elements averaged 0.42 to 0.76%. Altering the pH of the multi-element solution from 4.05 to 5.33, represented as the purple bar, yielded a significant change in adsorption efficiency values for scandium and the other rare earths. Scandium adsorption efficiency increased from 45% to 96.7% while the other rare earths averaged 10 to 14% except for Yttrium which had the lowest value at 5%.

The rare earths, Sc and Y, have similar adsorption values for their single element experiments but their adsorption efficiency values diverge when combined with other rare earth elements because much larger adsorption efficiency values were observed for Sc than Y, 96.7% vs 5% when the pH was changed to 5.33. The multi-element adsorption efficiency values suggest that it may be possible to selectively extract Scandium over other rare earths by controlling the pH. A possible explanation for this behavior may be due to the unique speciation of Scandium in an aqueous environment whereas most rare earth elements for the given pH values used in these experiments, will speciate as M^{+3} but scandium forms multiple hydroxide species over this range [41], [42]. Each scandium hydroxide species can interact with MNPs differently.

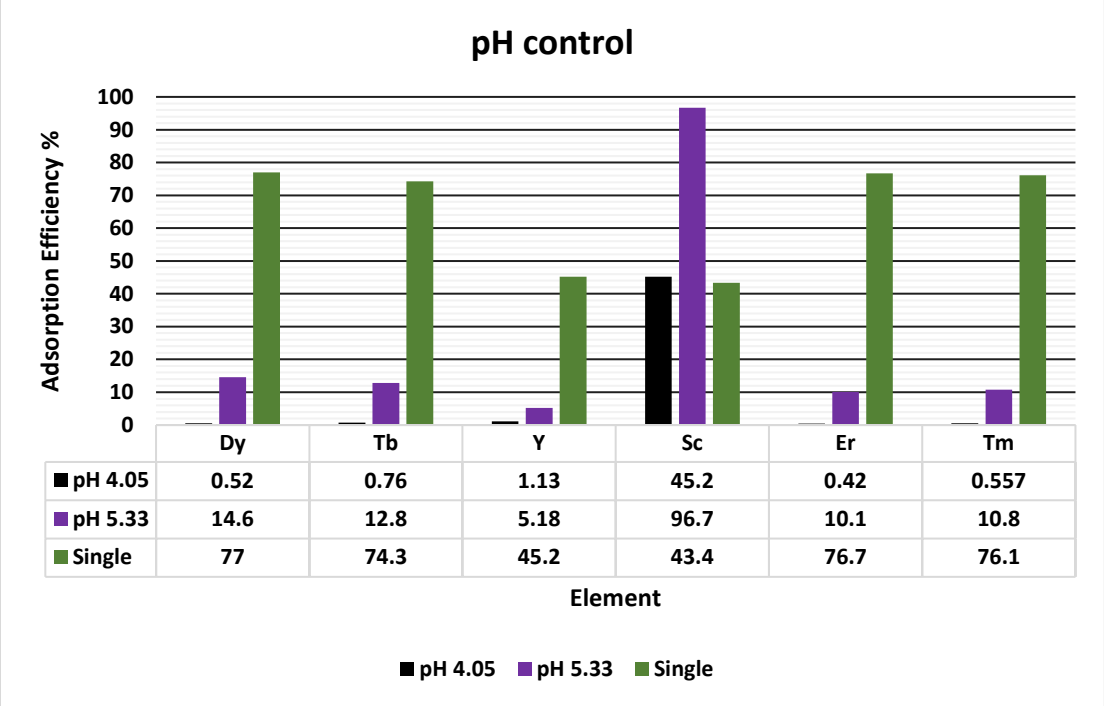

	Dy	Tb	Y	Sc	Er	Tm
pH 4.05	0.52	0.76	1.13	45.2	0.42	0.557
pH 5.33	14.6	12.8	5.18	96.7	10.1	10.8
Single	77	74.3	45.2	43.4	76.7	76.1

Figure 21: Data for the multi rare earth element MNP adsorption studies in which 250 mL of 100 ppm solution was mixed with 3.5 g of MNPs for 1 hr after adjusting the natural pH of the solution from 4.05 to 5.33

Rare earth multi-element (Dy, Tb, Y, Er, Tm) MNP control experiment results are displayed in Figure 22. The objective of these experiments was to determine if MNP dosage affected the selectivity of these rare earth elements. Therefore, increased MNPs additions of 7.0 g and 10.5 g were used instead of the standard 3.5 g. The pH was not adjusted and remained at its intrinsic value of 5.47. Mixing time was set to 1-hour.

In the 7.0 g MNP dose experiments Dy, Tb, and Tm averaged the highest adsorption efficiency values ranging from 41% to 47% where Tb had the highest adsorption efficiency value. Yttrium had the lowest adsorption efficiency value at 23% and Er had the second lowest adsorption efficiency value at 38%. Results from the 10.5 g MNP experiments show Dy, Tb, and Tm with the highest average of adsorption efficiency values ranging from 59% to 66% with Tb at the highest and Y the lowest. Yttrium and erbium have the lowest adsorption efficiency values

of 36% and 57%, respectively. Increasing the MNP dosage by 50% yielded an average improvement of adsorption efficiency value by approximately 50% for each element. No change in selectivity was observed by altering the MNP dosage between these rare earth elements.

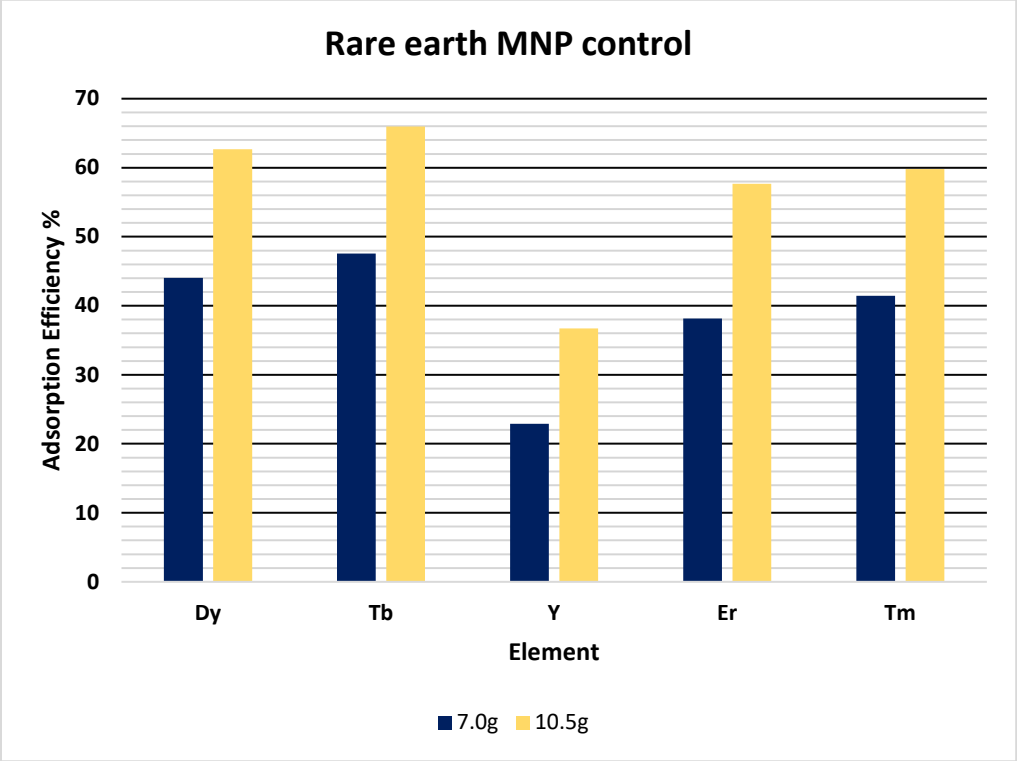

Figure 22: Adsorption efficiencies attained in the multi rare earth element MNP adsorption studies in which 250 mL of 100 ppm solution was mixed with 7.0 g of MNPs for 1-hr at the natural pH of the solution (5.47).

Figure 23 represents the data collected from the scandium kinetics study where the purpose was to establish a reference of time for the equilibrium of MNP with Sc to occur and to compare it with the multi-element kinetics study shown in Figure 24. The experiment begins with 750 mL of ~113 ppm Sc solution mixed with 10.5 g of MNPs. Samples of solution were taken periodically over the 1-hour duration. The pH was left at its intrinsic value of ~4.

At the end of the experiment approximately 41% of the starting ion concentration is sequestered by MNPs. The most significant changes in scandium concentration occur within the

first 100 seconds as the starting 113 ppm drops to 88.6 while gradual changes in concentration occur over the next 1000 seconds. Adsorption efficiency values agree with the non-kinetics single element study of Sc from Figure 20, where ~41% was recorded over the 1-hour duration.

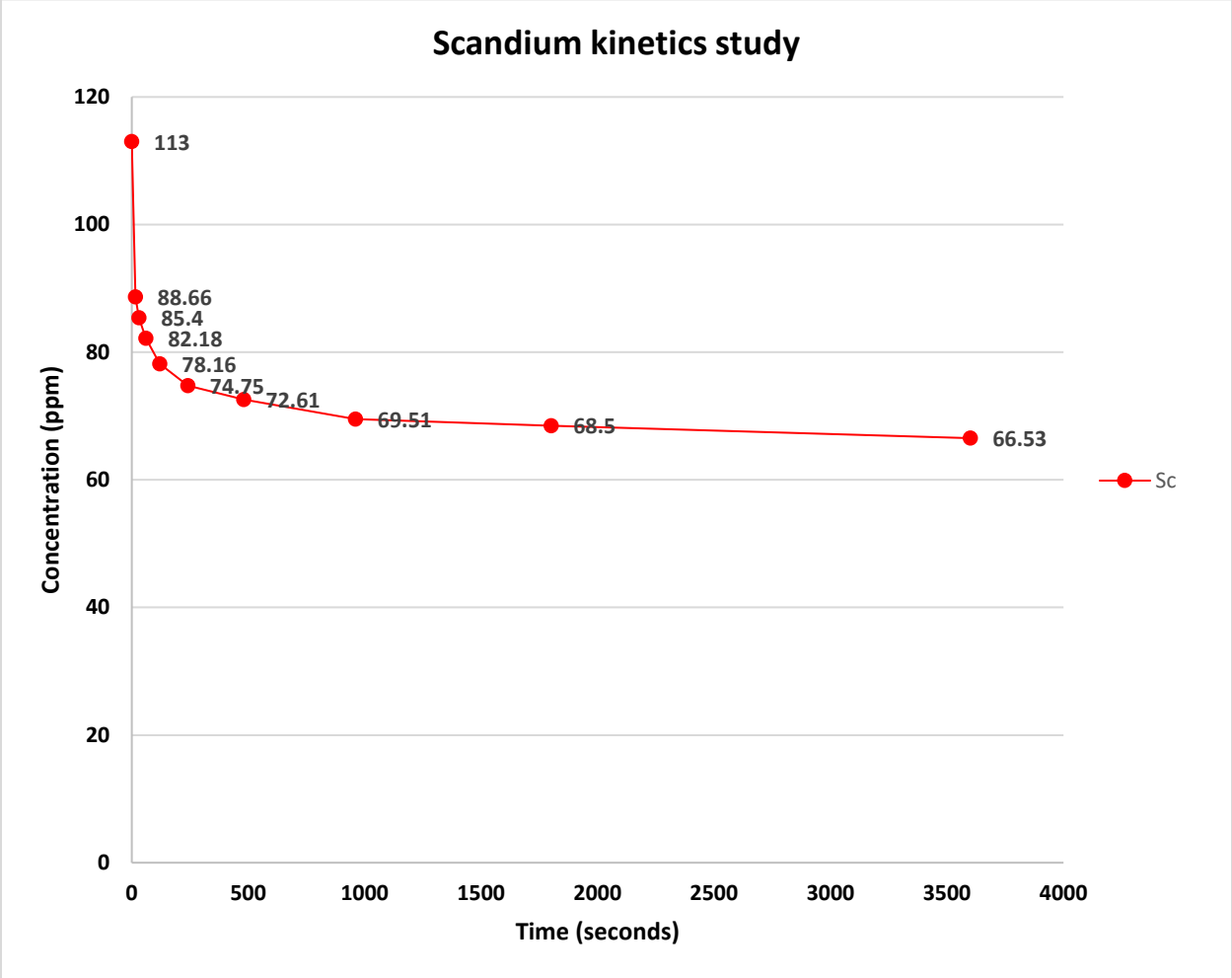

Figure 23: Concentration of scandium at various time intervals during 1 hr kinetics study of MNP adsorption. 10.5 g of MNP were mixed with 750ml of solution

Figure 24 represents the data collected from the scandium kinetics study with the purpose of investigating the change in concentration of scandium over time in a multiple rare earth element environment. Solutions of 750 mL at ~100 ppm concentration of each rare earth

element (Dy, Er, Sc, Tb, Tm, Y) were mixed with 10.5 g of MNPs and samples of solution taken periodically over a 1-hour period. The pH was left at its intrinsic value of ~4.

At the end of the 1-hour experiment, all the rare earths except for scandium exhibited an average of 4-6% adsorption efficiency values while scandium showed a substantially larger adsorption efficiency value of 72%. As with the single element kinetics study of scandium, the most significant changes in concentration occur within the first 100 seconds of the experiment with gradual changes over the following 1000 seconds. The exceptional adsorption efficiency value of scandium over the other rare earth elements suggests a strong selectivity.

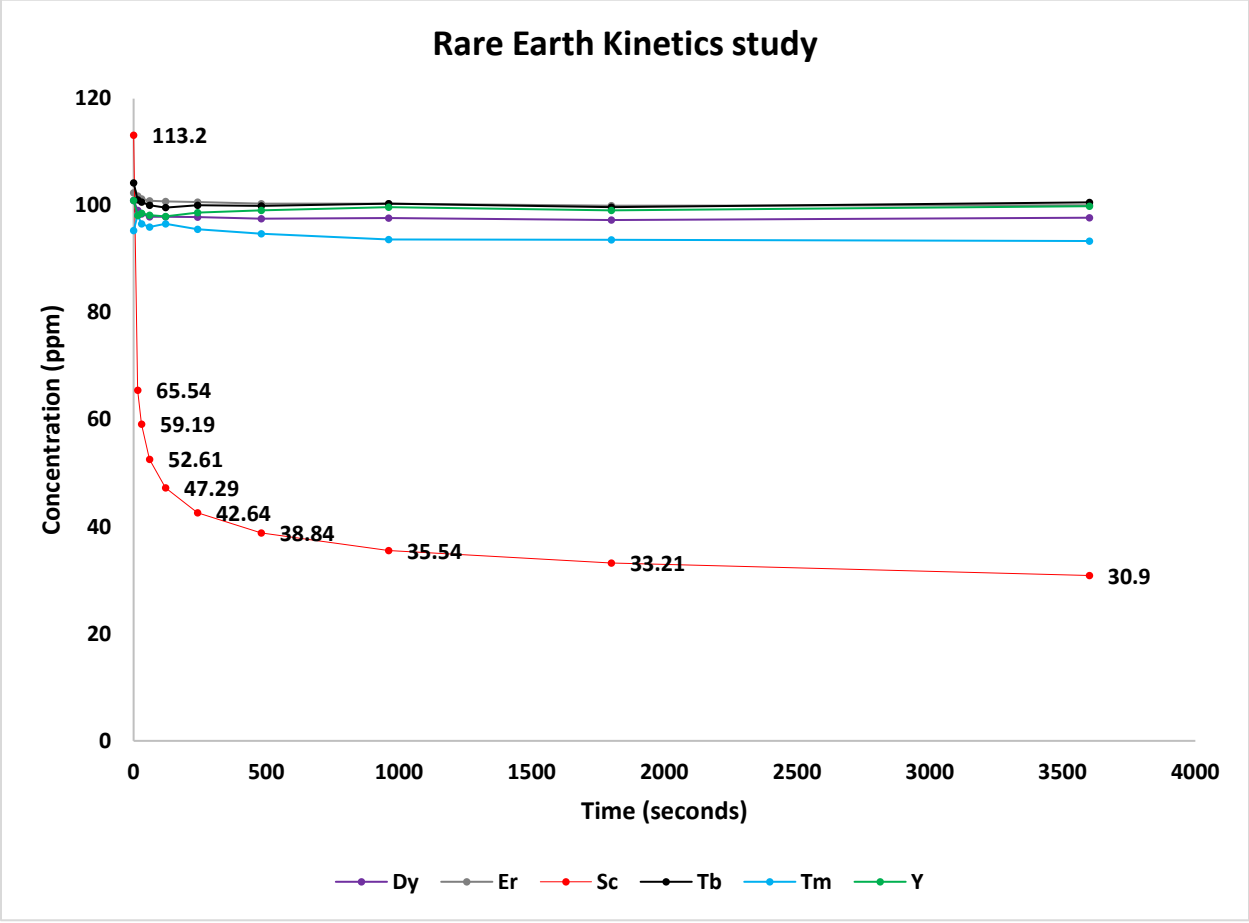

Figure 24: Concentration of multiple rare earths vs time in 1-hr kinetics study of MNP adsorption. In each case, 10.5 g of MNP were mixed with 750 ml of solution

Table 9 displays the calculated K_d and $K_{Sc(III)/M}$ values from Figure 21 in the experiments where pH was adjusted to 5.3. Scandium had the highest K_d value of all the rare earths involved in the experiment at a K_d value of 2100 mL/g MNPs. Yttrium had the lowest K_d value of 3.9, with Er and Tm at 8.0 to 8.6 mL/g MNPs, respectively. The K_d value of Tb was 10.4 and Dy at 12.2 mL/g. The selectivity coefficient values, $K_{Sc(III)/M}$, suggest that Yttrium will be the least competitive over the other rare earths for Sc uptake because it has the lowest value at 0.001 while the other rare earths average about 0.003 to 0.005. Based on the K_d values, selectivity for Sc is strong for pH values between 4 and 5 and the predicted selectivity order of these rare earths for would be:

Sc>>>Dy~Tb>Tm~Er>Y

Table 9 The Affinity of MNPs for Sc(III) and other coexisting rare earth ions in aqueous solution

Element	K_d, mL g^{-1}	$K_{Sc(III)/M}$
Dy	**12.2**	**0.005**
Tb	**10.5**	**0.004**
Y	**3.90**	**0.001**
Sc	**2100**	**1**
Er	**8.1**	**0.003**
Tm	**8.6**	**0.004**

Table 10 summarizes strontium adsorption data. Strontium was examined primarily because of its significance in the Butte mine waters. In addition to assessing strontium adsorption and loading capacity, the ability to strip adsorbed strontium ions was investigated. These experiments involved a surrogate solution of approximately 100 ppm Sr prepared by the dissolving of strontium-chloride salts. The pH was left at its intrinsic value and 250 mL of

solution was mixed with 3.5 g of MNP for one hour. After mixing, approximately 5 mL of sample was taken for ICP analysis while the remaining solution had its pH adjusted to approximately 0.84 and mixed for 20 minutes to remove any adsorbed Sr ions.

The single element experiments resulted in an adsorption efficiency of 23% with a loading capacity of 0.02 mmol/g of MNPs. Removing the adsorbed Sr ions showed minimal loss in adsorption efficiency with a value of 7%.

Table 10: Single element strontium, MNP adsorption and stripping studies. Surrogate solutions of 250mL of 100ppm were mixed with 3.5g of MNPs for 1 hr at the natural pH. The pH was then adjusted to ~0.84 and mixed for ~20 minutes to strip any adsorbed ions

Adsorption	Element	Initial Concentration (ppm)	Final Concentration (ppm)	Average mmol/g MNPs removed	Removal efficiency
	Sr	107	83	0.02	23
Stripping Recovery	Element	Initial Concentration (ppm)	Final Concentration (ppm)	Average mmol/g MNPs recovered	Recovery loss
	Sr	107	100	0.01	7

3.3. REE Ore experiments

The objective of the REE ore concentrate experiments was to evaluate surrogate solutions with concentrations similar to REE ore concentrate obtained from Bear Lodge for selectivity and, if selective behavior was observed, determine the effects of varying key experimental parameters such as MNP dosage, initial ion concentration, and pH. After the preliminary studies were completed, additional selectivity experiments were performed on a leach liquor from an actual REE ore concentrate sample that had been subjected to the chlorination roasting process.

Table 11 data are from adsorption experiments performed on single-element solutions. Single-element surrogate solutions of approximately 100 ppm and 1000 ppm were prepared from

chloride-based compounds for the REE (Ce, La, Gd, Dy) and gangue elements (Fe(II) and Ca). The pH of each solution was not adjusted and 3.5 g of MNP was added to solution and mixed for 1-hr before removal. High and low ion concentrations were used to determine how ion concentration affected loading capacity. Iron was omitted from the 1000 ppm experiments because the projected concentration values in the leach liquor are 20,000 ppm and above.

In the 100 ppm experiments, Gd and Dy had the highest adsorption efficiency values of approximately 76% each while Ce was the next highest at 68% adsorption and La was last of the REEs with an adsorption efficiency of 65%. Gangue element adsorption efficiency performance showed Fe(II) at 63% and Ca at 14%. The corresponding loading capacity values (mmol removed/g of MNP) was highest for Fe(II) at 0.07 then Dy at 0.04, Ce at 0.04, Gd at 0.04, La at 0.04, and finally Ca at 0.03.

The adsorption values for the 1000 ppm experiments showed Gd with the highest adsorption efficiency at 12% followed closely by Dy at 11%, La at 9% and Ce at 5%. Ca had an adsorption efficiency value of 3%. Gd had the highest loading capacity value of 0.06, then Ca at 0.06, La and Dy were similar with values of approximately 0.05 and Ce last at 0.03.

Single element adsorption efficiency and loading capacity values can be used as a reference for future multi-element experiments. The moderate adsorption efficiency values suggest that MNP each of the REEs tested could be recovered through multiple adsorption cycles. Adjusting the ion concentration affected the adsorption efficiency and loading capacity values for the REEs and Ca. The REEs have similar loading capacity values of approximately 0.04 mmol/g MNPs at the lower concentrations but increasing to a concentration of 1000 ppm yields La, Gd, and Dy with similar values of 0.06 while Ce is lower at a value of 0.03. A possible explanation for this behavior

is the increased competition from Cl ions which compete strongly against Ce for MNP adsorption compared to the other REEs.

Gangue element adsorption efficiency is likely to affect REE adsorption efficiency because Fe(II) had a higher loading capacity value at 0.07 compared to the REEs which averaged 0.04 for the 100 ppm experiments. While Ca had a significantly lower adsorption efficiency value than the REEs, it still had a comparable loading capacity value, suggesting that at those pH values and concentrations, Ca will compete with REEs adsorption efficiency.

Table 11: Single element REE ore surrogate solution adsorption studies. 3.5 g of MNPs were added to 250 mL of varying ion concentrations and mixed for 1-hr at the intrinsic pH

Experiment Set	Element	Initial Concentration (ppm)	Final Concentration (ppm)	Average mmol/g MNPs removed	Removal %	Initial pH	Final pH
100 ppm	Ce	109	35	0.04	68	4.96	5.24
	La	110	38	0.04	65	5.16	5.38
	Gd	106	25	0.04	76	5.08	5.25
	Dy	117	27	0.04	77	5.17	5.2
	Fe	91	33	0.07	63	2.47	3.24
	Ca	103	88	0.03	14	5.8	6.1
1000 ppm	Ce	1068	1004	0.03	6	5.6	5.1
	La	1122	1016	0.05	9	5.8	5.3
	Gd	1027	898	0.06	12	5.7	5.2
	Dy	1044	920	0.05	12	5.5	5.1
	Ca	986	955	0.06	3	9.5	5.1

Based on the results from the single element experiments of Table 11, the next experiments focused on determining how MNPs would adsorb the given elements in a multi-element solution at certain pH values and if changing the pH would affect the selectivity. Results are reported in Figure 25 and Table 12, where select data from Table 12 is graphically represented in Figure 25.

The pH values were chosen based on the average pH value of the single element REEs solutions (~5.01) and the pH value of the Fe(II) solution (~2.47). Surrogate solutions of approximately 100ppm were created from chloride-based compounds of the desired REEs, Fe(II), and Ca and mixed with 3.5 g of MNP for 1-hr.

The REEs had an average adsorption efficiency value of 5% from the low pH experiment and Ca had a value of 6% while Fe(II) had the highest at 60%. The REEs did not have significantly different loading capacity values and averaged 0.002 mmol/g MNPs. Fe had the highest loading capacity of 0.06 and Ca had a value of 0.01 mmol/g MNPs.

In the experiments where the pH was adjusted to 5.0, the REEs had adsorption efficiency values of 42, 40, 37, and 21% for Dy, Gd, Ce, and La, respectively. Altering the pH to 5.01 caused the iron to precipitate out of solution. Ca had an adsorption efficiency value of 0.42%. The loading capacity values from the pH 5.01 experiment for the REEs were 0.02, 0.02, 0.02, and 0.01 for Dy, Gd, Ce, and La, respectively. Ca had the lowest loading capacity value, 0.008, at the higher pH.

At the pH value of 2.47, the REEs did not differ greatly enough in loading capacity or adsorption efficiency values to indicate selectivity or favorable parameters for adsorption of REEs using MNP. The results for MNP adsorption of Fe(II) at a pH of 2.47 showed larger adsorption efficiency and loading capacity values compared to the REEs and Ca, suggesting that MNP will preferentially adsorb Fe(II) under those conditions. Increasing the pH to 5.01 yielded results more favorable for the adsorption of REEs. While Ce, Dy, and Gd have similar adsorption efficiency and loading capacity values at pH 5.01, La performed about half as well as the other REEs in terms of these parameters, indicating that MNP would be more likely to remove Ce, Gd, or Dy, over La for these conditions. Additionally, changing the pH to 5.01 greatly decreased Ca adsorption efficiency, allowing the removal of most of the REEs before Ca.

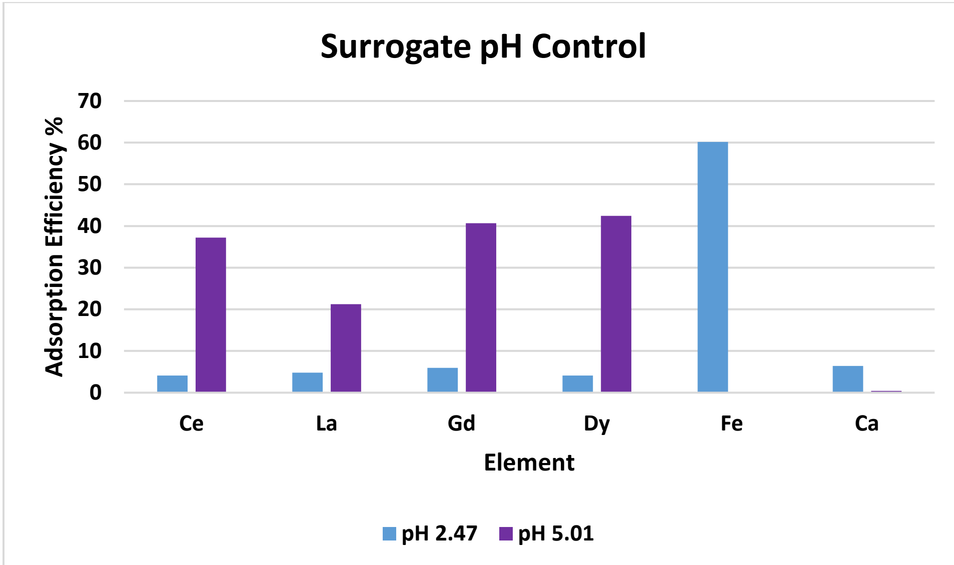

Figure 25: MNP adsorption of REEs and gangue elements study on the effect of pH. 3.5 g of MNPs were added to 250mL of surrogate solution and mixed for 1-hr at a starting pH of 2.47 and 5.01

Table 12: Tabulated data from Fig 25, MNP adsorption of REEs and gangue elements study on the effect of pH

[illegible]	[illegible]	[illegible]	[illegible]	[illegible]	[illegible]	[illegible]
[illegible]	[illegible]	[illegible]	[illegible]	[illegible]	[illegible]	[illegible]
[illegible]	[illegible]	[illegible]	[illegible]	[illegible]		
[illegible]	[illegible]	[illegible]	[illegible]	[illegible]		
[illegible]	[illegible]	[illegible]	[illegible]	[illegible]		
[illegible]	[illegible]	[illegible]	[illegible]	[illegible]		
[illegible]	[illegible]	[illegible]	[illegible]	[illegible]		
[illegible]	[illegible]	[illegible]	[illegible]	[illegible]	[illegible]	[illegible]
[illegible]	[illegible]	[illegible]	[illegible]	[illegible]		
[illegible]	[illegible]	[illegible]	[illegible]	[illegible]		
[illegible]	[illegible]	[illegible]	[illegible]	[illegible]		
[illegible]	[illegible]	[illegible]	[illegible]	[illegible]		
[illegible]	[illegible]	[illegible]	[illegible]	[illegible]		

Figure 26 and Table 13 present data from experiments focused on determining how altering the ion concentration to levels representative of a real ore sample would affect the adsorption efficiency and loading capacity values of MNP adsorption. Another objective was to determine if the filtration of a high concentration of iron via precipitation would affect the concentration of REEs. Two surrogate solutions were created with REE and gangue element concentrations of a real ore-sample, one of the solutions (unfiltered) omitted iron while the other (filtered) added approximately 20,000 ppm of iron to solution, then removed the iron via pH adjustment and filtering. The pH of both solutions was adjusted to approximately 4 before 7.0 g of MNP was added and mixed for 1-hr. A larger quantity of MNP was used because of the increased solution concentration.

Due to the varying starting concentrations of each element, the adsorption efficiency values are less likely to be an indication of selectivity. In the unfiltered experiment, the REEs Dy and Gd, have the highest adsorption efficiency values at 19.7 and 15.9%, respectively, but they also had the lowest loading capacity values out of the REEs where Dy has 0.011 and Gd at 0.011 mmol/g MNP. Cerium had the highest loading capacity value of 0.053. Calcium had an adsorption efficiency value of 3.7% and a loading capacity of 0.023.

Starting concentrations of the REEs and calcium were greatly affected by the removal of iron from solution, lowering the initial concentrations of dysprosium and gadolinium from 253 and 315 to 9.99 and 28.14, respectively. The initial concentrations of lanthanum and cerium were affected by the filtering of iron. Only the calcium concentration remained unaffected by the filtering process. Loading capacity values for dysprosium, gadolinium, and cerium were decreased the most by the filtering process while calcium and lanthanum loading capacity values fluctuated slightly.

Adjusting the element concentrations to better match proportions found in the REE ore-sample made it difficult to determine selectivity for one element over another and separating the effect of concentration from it.

While dysprosium and gadolinium have the highest adsorption efficiency values for the unfiltered experiment, their loading capacity values are approximately a fifth of the amount MNP could adsorb for cerium, 0.054 mmol/g MNP. MNP adsorption of calcium in the unfiltered solution could be problematic for the selective adsorption of REEs over gangue elements since it has a loading capacity value greater than Dy and Gd in these conditions.

Higher adsorption efficiency values for dysprosium and gadolinium are to be expected with notably lowered starting concentrations and should not be interpreted as evidence of selectivity. The filtering process resulting in La having the highest concentration out of all the elements present, but the loading capacity value was similar to what was observed in the unfiltered experiment, 0.033 vs 0.35 mmol/g MNP, filtered vs unfiltered.

Calcium concentration was not affected by the filtering process and the loading capacity and adsorption efficiency values are similar even with a lower concentration of REEs, suggesting that MNP is not selective towards calcium but enough will still be removed and accumulated through multiple cycles in a real industrial application to affect REEs purity.

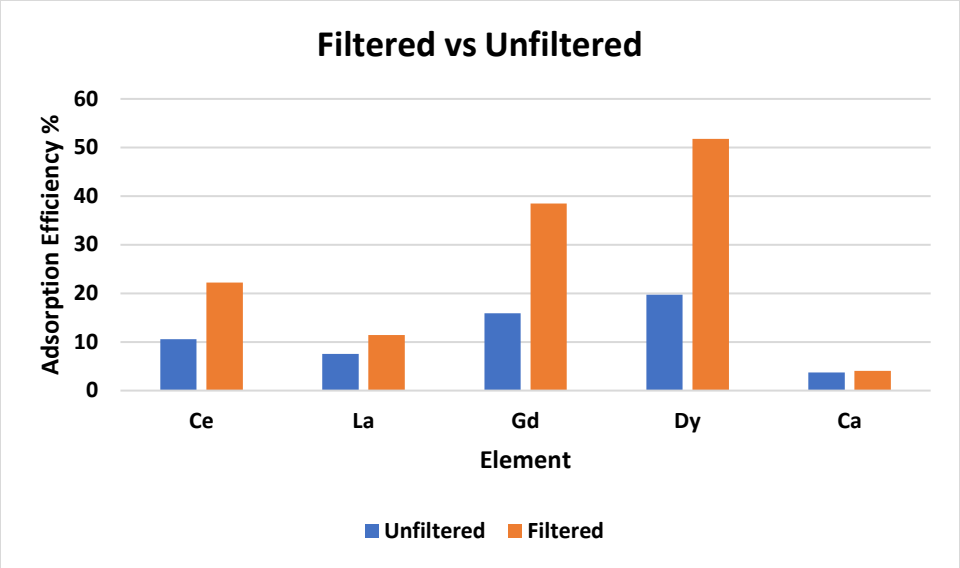

Figure 26: REE ore surrogate study on the effect of iron chloride to MNP. Two experiments were conducted, one had no iron chloride added and is marked as 'unfiltered'. The experiment where iron chloride was added then precipitated out of solution and filtered is marked as 'filtered'. 7.0g of MNPs were added to 250 mL of solution and mixed for 1-hr at the intrinsic pH

Table 13: Tabulated data from Fig 26 on the REE ore surrogate study on the effect of iron chloride to MNP

Unfiltered	Element	Initial Concentration (ppm)	Final Concentration (ppm)	Average mmol/g MNPs removed	Removal %	Initial pH
	Ce	1986	1775	0.05	10	4.03
	La	1817	1679	0.03	7	
	Gd	315	265	0.01	15	
	Dy	253	203	0.01	19	
	Ca	707	681	0.02	4	
Filtered	Ce	674	524	0.03	22	3.95
	La	1139	1008	0.03	11	
	Gd	28	17	0.002	38	
	Dy	10	5	0.001	51	
	Ca	710	681	0.02	4	

The effects of MNP dosage on selectivity were evaluated in Tables 14 and 15. These experiments examined adsorption efficiency and loading capacity values using three different MNP dosages: 0.88, 3.5, and 7.0 g. Approximately 250 mL of surrogate solution (made in ion concentrations representing the REE ore concentrate sample) were mixed with varying dosages of MNP for 1-hr at the intrinsic pH of the solution. After 1-hr the MNPs were extracted from the solution and an identical dosage was added to the solution and mixed for 1-hr to evaluate the effectiveness of multiple cycles on selectivity, adsorption efficiency, and loading capacity.

Table 14: Cycle_1 results of the REE ore surrogate solution. Varying dosages of MNPs (0.88 g, 3.5 g, and 7.0 g) were added to 250 mL of solution and mixed for 1-hr at the intrinsic pH

Cycle#1	Element	Initial Concentration (ppm)	Final Concentration (ppm)	Average mmol/g MNPs removed	Adsorption efficiency	Initial pH	Final pH	MNP(g)
	Ce	1999	1258	1.5	37	5.44	5.07	0.88
	La	1877	1519	0.7	19			
	Gd	59	23	0.06	60			
	Dy	52	14	0.06	71			
	Ca	763	768	0	0			
	Ce	1999	1222	0.40	38	5.2	5.24	3.5
	La	1877	1532	0.18	18			
	Gd	59	20	0.017	64			
	Dy	52	12	0.017	75			
	Ca	763	779	0	0			
	Ce	1999	1020	0.25	48	5.25	5.34	7
	La	1877	1391	0.12	25			
	Gd	59	13	0.01	76			
	Dy	52	8	0.01	83			
	Ca	763	799	###	###			

Cycle_1 results, Table 14, show a minimal increase in adsorption efficiency values across all types of the REEs when increasing MNP dosage to 3.5 g from 0.88 g, but a large increase in adsorption efficiency when the dosage is increased to 7.0 g. Changes in adsorption efficiency values for Ca are undetectable for all three MNP dosages in the first cycle. The loading capacity values should be evaluated with respect to the MNP dosage of the same value. In all MNP

dosages used Ce consistently has the highest loading capacity, and Dy has the highest adsorption efficiency value amongst the REEs.

Table 15: Cycle_2 results of the REE ore surrogate solution. MNPs from Cycle#1 were removed then varying dosages of MNPs (0.88 g, 3.5 g, and 7.0 g) were added to the remaining solution and mixed for 1-hr at the intrinsic pH.

Cycle#2	Element	Initial Concentration (ppm)	Final Concentration (ppm)	Average mmol/g MNPs removed	Removal efficiency	Initial pH	Final pH	MNP(g)
	Ce	1258	1191	0.136	5	5.07	5.12	0.88
	La	1519	1485	0.068	2			
	Gd	23.5	22.2	0.002	5			
	Dy	14.7	14.2	0.001	4			
	Ca	768	729	0.279	5			
	Ce	1222	1119	0.052	8	5.24	5.26	3.5
	La	1532	1472	0.031	4			
	Gd	20.7	17.8	0.001	13			
	Dy	12.9	11	0.001	13			
	Ca	779	770	0.016	1			
	Ce	1020	815	0.052	20	5.34	5.47	7
	La	1391	1241	0.038	10			
	Gd	13.9	9	0.001	31			
	Dy	8.4	6	0.0004	25			
	Ca	799	775	0.021	3			

Cycle_2 loading capacity and adsorption efficiency values, presented in Table 15, are lower than those reported in Cycle#1 for the REEs. Changes in calcium concentration were detectable and show the highest adsorption efficiency and loading capacity values using the lowest dosage of MNP. Unlike the results from Cycle_1, the change in adsorption efficiency values for the REEs increases greatly as MNP dosage increases. Gd and Dy have similar adsorption efficiency values until MNP dosage of 7.0 g, then Gd had a value of 31.1% and Dy a value of 25%. Cerium has the highest loading capacity value, 0.136 mmol/g of MNPs, compared to other REEs.

Adsorption efficiency values for REEs in Cycle_1 show promising results for the selective adsorption efficiency of REEs over calcium. Increasing the MNP dosage from 0.88 g to 3.5 g did not provide the expected substantial increase to adsorption efficiency as in previous cases with MNP control experiments; rather, only after increasing MNP dosage to 7.0 g does the adsorption efficiency change meaningfully. It is possible that the adsorption efficiency values for the REEs display little difference between 0.88 g and 3.5 g of MNP because only a portion of the REEs are adsorbed by the MNPs before the excess of chlorine ions compete with the remaining REEs. Only 7.0 g of MNP showed further increase to adsorption efficiency values of REEs because of an excess of available adsorption sites. Based on the lowest loading capacity and adsorption efficiency values for La, it appears that La ions are less competitive than the other REEs for available MNP adsorption sites.

Calcium adsorption efficiency increases significantly during Cycle_2, having loading capacity values of 0.28 mmol/g MNP while the highest REE loading capacity using 0.88 g of MNP was 0.137 mmol/g MNP for Ce. The competitiveness of Ca over the REEs, particularly Dy and Gd, is present at all MNP dosages. Lanthanum remains the least competitive REE at all three MNP dosages during Cycle_2. Adsorption efficiency and loading capacity values are significantly lower than Cycle_1, which may be due to residual MNP from the previous cycle and a change in overall ion concentration.

Table 16 represents the data collected from an experiment where varying dosages of MNPs were added to diluted leach liquor from a REE ore concentrate. The pH was left at its intrinsic value and the iron was left in solution. A smaller total volume of 12.5 mL was used because of the limited quantity of leach liquor available.

No changes in the REEs were measured at any of the MNPs dosages. Unprecipitated iron most likely saturated the MNPs before the REEs could be adsorbed. Estimated concentrations of iron before leach liquor dilution averaged around 20,000 ppm while the highest rare earth concentration was estimated to be at approximately 8000 ppm. The data collected assisted in the design of future experiments, particularly an emphasis on diluting the leach liquor and removal of as much iron as possible for adsorption of REEs to occur.

Table 16: Leach liquor from REE ore chloride roasting adsorption results. Stock liquor solution was diluted by ½ of original concentration before beginning experiment. Each experiment used 12.5 mL of solution with varying concentrations of magnetite (0.175 g, 0525 g, 1.75 g) that were mixed for 1-hr

	Ce(ppm)	Dy(ppm)	Gd(ppm)	La(ppm
Leach Stock	**4608**	**432**	**129**	**4548**
0.175 g of MNP	**4633**	**438**	**131**	**4584**
0.525 g of MNP	**4572**	**433**	**129**	**4516**
1.75 g of MNP	**4549**	**432**	**129**	**4529**

Table 17 represents the data collected from MNP adsorption of REE ore leach liquor that was diluted by ¼ its original concentration and pH adjusted to precipitate and filter iron from the solution. Solution volume was adjusted, keeping the same proportions of 250 mL and 3.5 g of MNPs but scaled down to 6.25 mL and 0.0875 g.

At a dosage of 0.0875 g of MNPs, Ce had the highest removal compared to the other REEs. No changes in Dy concentration were measured. The element with the highest adsorption efficiency was Fe at 24%. Adjusting the MNP dosage to 0.175 g increased the adsorption efficiency of Fe from 24 to 45%, Ce from 3.3 to 8% and an increase for the other REEs. At both MNP dosages there was no change observed in Ca concentration.

Even with a much higher concentration than iron, 1380 ppm for Ce and 197 ppm for Fe, the MNPs adsorbed more Fe than Ce and La. The data suggests that MNPs will preferentially adsorb iron over REEs at a pH of 4.4; while calcium is nonselective in these conditions.

Table 17: Changes in ion concentration and adsorption efficiencies from the REE ore leach liquor experiment. Stock leach liquor was diluted by ¼ then pH raised with 10% NaOH solution to precipitate Fe. The precipitates were filtered out and the pH of the starting solution was 4.43. 6.25 mL of solution were mixed with 0.0875 g and 0.175 g of MNPs for 1-hr

	Initial pH: 4.43					
	Final pH 4.51			Final pH 4.57		
	MNP dosage: 0.0875g			MNP dosage: 0.175g		
Element	Initial Concentration (ppm)	Final Concentration (ppm)	% removed	Initial Concentration (ppm)	Final Concentration (ppm)	% removed
Fe	197	149	24	197	107	45
Ca	151	153	0	151	159	0
Ce	1380	1334	3	1380	1269	8
Dy	65.3	65	0	65.3	65	0.12
Gd	7.1	6.8	3	7.123	6	7
La	1878	1875	0.16	1878	1836	2.21

4. Conclusions and future work

4.1. Conclusions

The findings in this study show that virgin MNPs, a cost-effective and environmentally safe adsorbent, has potential to be used for the selective removal of Cr(III), Sc(III), and iron. Findings and conclusions supported by the collected data are as follows:

Virgin MNPs will selectively adsorb Cr(III) over a range of REEs and bivalent metals and this selectivity is adjustable by altering the MNPs dosage and pH. A constant solution pH of 4.45

or a starting pH of 3.36 (not held constant) yielded the most favorable results for selective chromium adsorption over other metal ionic species. Adjusting the MNPs dosage to lower values yields a high adsorption efficiency of chromium and loading capacity values compared to the competing ionic species of REEs and heavy metals. The selective behavior of chromium suggests that virgin MNPs could be used for its selective adsorption over competing REEs, heavy metals, and gangue constituents and the MNP selectivity was determined as follows:

$$Cr(III) >> La(III) > Cu(II) >> Cd(II) > Co(II)$$

The REEs study showed that virgin MNPs can adsorb most of the REEs and multiple adsorption cycles could result in near-complete removal. Scandium was found to competitively adsorb in preference to other REEs. The selectivity for scandium is pH-dependent, achieving higher adsorption efficiencies at a pH range of 5.3 and lower efficiencies at a pH of 4.1. At both pH conditions of 5.3 and 4.1, scandium adsorption efficiency was greater than the other REEs. The MNP selectivity for selected REEs was determined as follows:

$$Sc >>> Dy \sim Tb > Tm \sim Er > Y$$

Studies using chlorinated rare earth ore concentrate surrogate solutions and actual sample solutions studies revealed the competitive adsorption behavior of iron over REEs. When at similar ion concentrations, the selectivity for iron is prevalent at a low pH (2.47) while REE adsorption efficiency is significantly lower. Filtering iron via precipitation was problematic in the surrogate and actual solution samples because of the significant removal of REE concentration as well. In the adsorption studies using leach liquor from an actual chlorinated REE ore concentrate, iron was selectively adsorbed in preference to the REEs and calcium. Surrogate solutions and actual sample solutions show that calcium does not selectively adsorb over the REEs at a pH of 5.01 or 4.5.

4.2. Future work

Further studies devoted to an improved understanding of the adsorption and ionic speciation behavior of Cr(III) and Sc(III) would be beneficial. A potential area for further work would be studying how the presence of multiple elements affects the stripping of adsorbed species. Additionally, studies on measuring the effects of non-metal species (such as chloride and sulfates) on the adsorption of metal ions is needed. The development of treating REE ore leach liquor needs to be investigated, specifically the removal of iron while preserving REE concentrations.

Research on how unequal starting concentrations, to better mimic real solutions, would affect the adsorption and selectivity trends observed in this study should be investigated. The adaption and scaling of the findings in this study to the CFMR system for potential use in an industrial process will require additional research. Experiments in this study were done typically using single-cycle adsorption but real application will likely require multiple cycles to treat the target ions in aqueous solution. The REE ore adsorption cycle experiment showed an unexplained change in adsorption behavior between the cycles and warrants further investigation. Examining the effects of other gangue elements, such as Sr and Na, for any potential selectivity behavior and how their presence would affect the adsorption of desired metals. Temperature was not a parameter investigated in this study and further research on its effects on selectivity would be beneficial. The effects of REEs interaction on ionic activity is an area of interest to better understand the molecular interactions influencing selective adsorption.

5. Bibliography

[1] Casarett and Doull, *Toxicology The basic Science of Poisons*, 9th ed. McGraw Hill Education.

[2] M. A. Ahmed, S. M. Ali, S. I. El-Dek, and A. Galal, "Magnetite-hematite nanoparticles prepared by green methods for heavy metal ions removal from water," *Mater Sci Eng B Solid State Mater Adv Technol*, vol. 178, no. 10, pp. 744–751, Jun. 2013, doi: 10.1016/j.mseb.2013.03.011.

[3] L. Leyssens, B. Vinck, C. Van Der Straeten, F. Wuyts, and L. Maes, "Cobalt toxicity in humans—A review of the potential sources and systemic health effects," *Toxicology*, vol. 387. Elsevier Ireland Ltd, pp. 43–56, Jul. 15, 2017. doi: 10.1016/j.tox.2017.05.015.

[4] L. Leyssens, B. Vinck, C. Van Der Straeten, F. Wuyts, and L. Maes, "Cobalt toxicity in humans—A review of the potential sources and systemic health effects," *Toxicology*, vol. 387. Elsevier Ireland Ltd, pp. 43–56, Jul. 15, 2017. doi: 10.1016/j.tox.2017.05.015.

[5] Ruth F Schulte, "U.S. Geological Survey," Mineral Commodity.

[6] P. Liang and W. Fa, "Determination of La, Eu and Yb in water samples by inductively coupled plasma atomic emission spectrometry after solid phase extraction of their 1-Phenyl-3-methyl-4-benzoylpyrazol-5-one complexes on silica gel column," *Microchimica Acta*, vol. 150, no. 1, pp. 15–19, May 2005, doi: 10.1007/s00604-005-0340-9.

[7] C. Liu *et al.*, "Bioaccessibility and health risk assessment of rare earth elements in Porphyra seaweed species," *Human and Ecological Risk Assessment*, vol. 24, no. 3, pp. 721–730, Apr. 2018, doi: 10.1080/10807039.2017.1398070.

[8] K. T. Rim, K. H. Koo, and J. S. Park, “Toxicological evaluations of rare earths and their health impacts to workers: A literature review,” *Safety and Health at Work*, vol. 4, no. 1. Elsevier Science B.V., pp. 12–26, 2013. doi: 10.5491/SHAW.2013.4.1.12.

[9] D. Cai and Y. kui Rui, “Determination of rare earth elements in Camellia oleifera seeds from rare earth elements mining areas in Southern Jiangxi, China by ICP-MS,” *Journal fur Verbraucherschutz und Lebensmittelsicherheit*, vol. 6, no. 3, pp. 349–351, Sep. 2011, doi: 10.1007/s00003-010-0650-7.

[10] A. B. Botelho Junior, D. C. R. Espinosa, J. Vaughan, and J. A. S. Tenório, “Recovery of scandium from various sources: A critical review of the state of the art and future prospects,” *Minerals Engineering*, vol. 172. Elsevier Ltd, Oct. 01, 2021. doi: 10.1016/j.mineng.2021.107148.

[11] D. Hutchins, “Digital Commons @ Montana Tech CONTINUOUS FLOW PROCESS FOR RECOVERY OF METAL CONTAMINANTS FROM INDUSTRIAL WASTEWATERS WITH MAGNETIC NANOCOMPOSITES.” [Online]. Available: https://digitalcommons.mtech.edu/grad_rschhttps://digitalcommons.mtech.edu/grad_rsch/183

[12] S. Sarode *et al.*, “Overview of wastewater treatment methods with special focus on biopolymer chitin-chitosan,” *International Journal of Biological Macromolecules*, vol. 121. Elsevier B.V., pp. 1086–1100, Jan. 01, 2019. doi: 10.1016/j.ijbiomac.2018.10.089.

[13] F. I. El-Dib, D. E. Mohamed, O. A. A. El-Shamy, and M. R. Mishrif, “Study the adsorption properties of magnetite nanoparticles in the presence of different synthesized surfactants for heavy metal ions removal,” *Egyptian Journal of Petroleum*, vol. 29, no. 1, pp. 1–7, Mar. 2020, doi: 10.1016/j.ejpe.2019.08.004.

[14] M. Namdeo, "Magnetite Nanoparticles as Effective Adsorbent for Water Purification-A Review," *Advances in Recycling & Waste Management*, vol. 02, no. 03, 2018, doi: 10.4172/2475-7675.1000135.

[15] S. L. Iconaru, R. Guégan, C. L. Popa, M. Motelica-Heino, C. S. Ciobanu, and D. Predoi, "Magnetite (Fe3O4) nanoparticles as adsorbents for As and Cu removal," *Appl Clay Sci*, vol. 134, pp. 128–135, Dec. 2016, doi: 10.1016/j.clay.2016.08.019.

[16] E. Ghasemi, A. Heydari, and M. Sillanpää, "Superparamagnetic Fe3O4@EDTA nanoparticles as an efficient adsorbent for simultaneous removal of Ag(I), Hg(II), Mn(II), Zn(II), Pb(II) and Cd(II) from water and soil environmental samples," *Microchemical Journal*, vol. 131, pp. 51–56, Mar. 2017, doi: 10.1016/j.microc.2016.11.011.

[17] R. C. Popescu, E. Andronescu, and B. S. Vasile, "Recent advances in magnetite nanoparticle functionalization for nanomedicine," *Nanomaterials*, vol. 9, no. 12. MDPI AG, Dec. 01, 2019. doi: 10.3390/nano9121791.

[18] S. A. Elfeky, S. E. Mahmoud, and A. F. Youssef, "Applications of CTAB modified magnetic nanoparticles for removal of chromium (VI) from contaminated water," *J Adv Res*, vol. 8, no. 4, pp. 435–443, Jul. 2017, doi: 10.1016/j.jare.2017.06.002.

[19] G. Wallace, "Digital Commons @ Montana Tech Optimization of Rare Earth Leaching from Ores and Concentrates." [Online]. Available: http://digitalcommons.mtech.edu/grad_rschhttp://digitalcommons.mtech.edu/grad_rsch/27

[20] D. L. Hutchins and J. P. Downey, "Effective separation of magnetite nanoparticles within an industrial-scale pipeline reactor," *Separation Science and Technology (Philadelphia)*, vol. 55, no. 15, pp. 2822–2829, Oct. 2020, doi: 10.1080/01496395.2019.1646762.

[21] Teagan J. Letizke, J. Downey, Richard M. LaDouceur, Daisy M. Margrave, Grant C. Wallace, and David L. Hutchins, "Water Treatment Method for Removal of Select Heavy Metals and Nutrient Ions Through Adsorption by Magnetite," *ACS Publications*, vol. 9, no. ACS EST Water, pp. 1584–1592, Aug. 2022.

[22] T. Leitzke, J. Downey, D. Hutchins, B. St Clair, and S. Clair, "Continuous Flow Metal Recovery System Using Magnetic Nanocomposites for Contaminated Waters." [Online]. Available: https://digitalcommons.mtech.edu/techxpo-event/13

[23] Mark Winter, "webelements.com," University of Sheffield, UK.

[24] Schweitzer A. P., *Handbook of Separation Techniques for Chemical Engineers*. James Peter Associates, Inc., 1979.

[25] A. D. Aderibigbe and A. J. Clark, "Novel N-(2-((4-vinylbenzyl)thio)ethyl)Acetamide Functionalized Magnetite Nanoparticle: Synthesis and Test Selective Silver(I) Removal Study," *J Inorg Organomet Polym Mater*, vol. 30, no. 11, pp. 4803–4808, Nov. 2020, doi: 10.1007/s10904-020-01716-1.

[26] D. Dupont, W. Brullot, M. Bloemen, T. Verbiest, and K. Binnemans, "Selective uptake of rare earths from aqueous solutions by EDTA-functionalized magnetic and nonmagnetic nanoparticles," *ACS Appl Mater Interfaces*, vol. 6, no. 7, pp. 4980–4988, Apr. 2014, doi: 10.1021/am406027y.

[27] L. Kostenko, N. Kobylinska, S. Khainakov, and S. G. Granda, "Magnetite nanoparticles with aminomethylenephosphonic groups: synthesis, characterization and uptake of europium(III) ions from aqueous media," *Microchimica Acta*, vol. 186, no. 7, Jul. 2019, doi: 10.1007/s00604-019-3520-8.

[28] Buchanan and Stacy, “EERE Technical Report Template,” 2022. [Online]. Available: www.energy.gov/policy/supplychains.

[29] V. B. Grass, “Rare Earth Elements in National Defense: Background, Oversight Issues, and Options for Congress,” Washington, DC, 2013.

[30] B. Venditti, “Visualizing the Critical Metals in a Smartphone,” TECHNOLOGY METALS.

[31] A. Cohen and J. Grant, “America’s Critical Strategic Vulnerability: Rare Earth Elements,” *Foreign Policy Research Institute*, Jun. 2021.

[32] MP Materials, “Rare Earth Elements.”

[33] Q. Tan, J. Li, and X. Zeng, “Rare Earth Elements Recovery from Waste Fluorescent Lamps: A Review,” *Critical Reviews in Environmental Science and Technology*, vol. 45, no. 7. Taylor and Francis Inc., pp. 749–776, Apr. 03, 2015. doi: 10.1080/10643389.2014.900240.

[34] N. Um, “Hydrometallurgical Recovery Process of Rare Earth Elements from Waste: Main Application of Acid Leaching with Devised τ-T Diagram,” in *Rare Earth Element*, InTech, 2017. doi: 10.5772/intechopen.68302.

[35] Rare Element Resources Ltd., “Rare Earth Element Resources.”

[36] C. Gupta and N. Krishnamurthy, *Extractive Metallurgy of Rare Earths*. Boca Raton: CRC Press, 2005.

[37] F. Habashi, “Extractive metallurgy of rare earths,” *Canadian Metallurgical Quarterly*, vol. 52, no. 3, pp. 224–233, Jul. 2013, doi: 10.1179/1879139513Y.0000000081.

[38] G. Meyer and P. Ax, “An Analysis of the Ammonium Chloride Route to Anhydrous Rare-Earth Metal Chlorides,” *Mater Res Bull*, vol. 17, no. 28, pp. 1447–1455, Sep. 1982.

[39] D. Gaede, “Digital Commons @ Montana Tech CHLORINATION AND SELECTIVE VAPORIZATION OF RARE EARTH ELEMENTS.” [Online]. Available: http://digitalcommons.mtech.edu/grad_rschhttp://digitalcommons.mtech.edu/grad_rsch/72

[40] “Gaede TMS 2015”.

[41] R. Kallio *et al.*, “Leaching characteristics of Sc-enriched, Fe-depleted acidic slags,” *Miner Eng*, vol. 189, Nov. 2022, doi: 10.1016/j.mineng.2022.107901.

[42] D. G. Brookins, S.-V. Berlin, H. New, Y. London, and P. Tokyo, “Eh-pH Diagrams for Geochemistry With 98 Figures and 61 Tables.”

Appendix A:

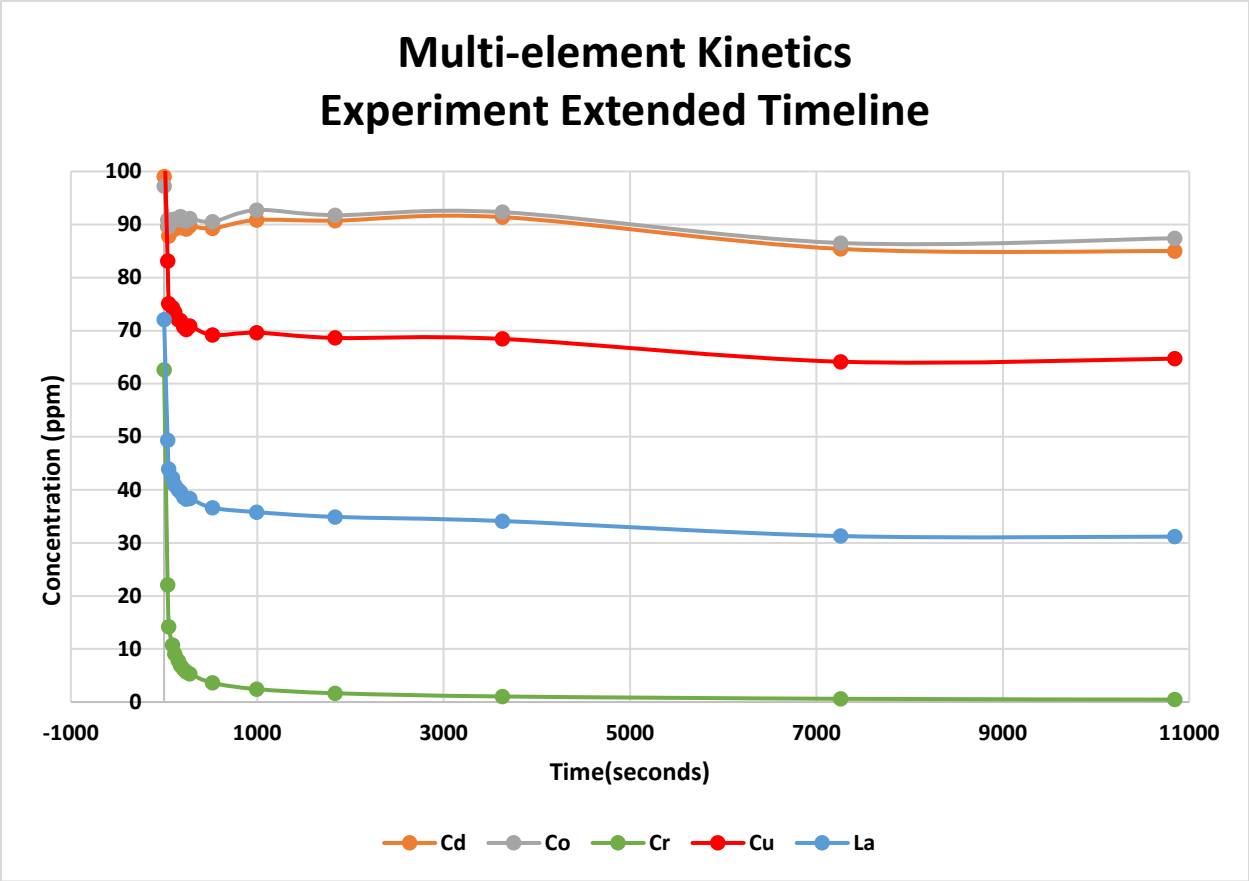

Figure 27: Change in concentration vs time for 450 mL of mixed surrogate solution mixed with 6.3 g of magnetite for 3 hours.

Table 18: Equilibrium pH values of single element experiments.

Single element experiment	Equilibrium pH values
Cd	6.2
Cr	5.7
Co	6.1
Cu	5.2
La(sulfate)	5.7
Sc	4
Dy	5.1
Gd	5.2
Ce	5.2
Er	5.4
Tb	5.3
Tm	5.4
Y	5.3
Yb	5.1
Pr	5.2
Fe	2.7
Ca	6.3
Mn	4.8
Zn	4.7
Al	5.3

Table 19: Equilibrium pH values of all experiments.

Experiment	Equilibrium pH value
Multi-element starting pH 4.43	5.2
Multi-element starting pH 3.36	5.1
MNP control Series_1 (dosage) 3.5 g	5.2
MNP control Series_1 (dosage) 2.33 g	4.8
MNP control Series_1 (dosage) 1.75 g	4.7
MNP control Series_1 (dosage) 1.17 g	4.5
Scoping MNP control Series_2 (dosage) 7 g	4.9
Scoping MNP control Series_2 (dosage) 3.5 g	4.3
Scoping MNP control Series_2 (dosage) 2.33 g	4.2
Scoping MNP control Series_2 (dosage) 1.75 g	4.1
Scoping MNP control Series_2 (dosage)1.17 g	4.1
Scoping Series_3 (varied element mixture) Fe	3.9
Scoping Series_3 (varied element mixture) Mn	4.4
Scoping Series_3 (varied element mixture) Zn	4.6
Scoping Series_3 (varied element mixture) Al	4.1
Scoping Series_3 (varied element mixture) Pr	5.2
Scoping Series_3 (varied element mixture) Dy	5.3
Rare earth element experiments (Sc, Gd, Yb, La)	3.9
Rare earth pH control (Initial 4.05)	5.9
Rare earth pH control (Initial 5.33)	6.1
Multi-REE (Dy, Tb, Y, Er, Tm) dosage 10.5 g	6.4
Multi-REE (Dy, Tb, Y, Er, Tm) dosage 7.0 g	6.1